



Republic of Iraq
Ministry of Higher Education and Scientific Research
University of Misan
College of Engineering
Department of Electrical Engineering



Design Control Circuit Of Active Power Filter

A Graduation Project
is Submitted to the Electrical Engineering Department / Engineering
College in Partial Fulfillment of the Requirements for the
Degree of Bachelor of Science
in Electrical Engineering

By

Jaafar Mohammed Saleh

Abbas Ali Khamas

Sajjad Hassan Madhboub

Baneen Hassan Hashim

Supervised

Assist. Prof. Dr. Jabbar Raheem Rashed

Misan, Iraq

2025

بِسْمِ اللَّهِ الرَّحْمَنِ الرَّحِيمِ

{ وَفَوْقَ كُلِّ ذِي عِلْمٍ عَلِيمٌ }

يوسف الآية (76)

صدق الله العليُّ العظيم

SUPERVISOR CERTIFICATION

I certify that the preparation of this project entitled (**Design Control Circuit of Active Power Filter**) prepared by (**Jaafar Mohammed Saleh, Abbas Ali Khamas, Sajjad Hassan Madhboub, Baneen Hassan Hashim**) was under my supervision at General Electrical Engineering Branch, Electrical Engineering Department, University of Misan in partial fulfilment of the requirements for the degree of Bachelor of Science in Electrical Engineering.

Signature:

Supervisor Name: Jabbar Rahim Rashid

Scientific Degree :Assistant Professor

Date:

CERTIFICATE OF EXAMINERS

We certify, as an examining committee, that we have read this project report entitled " **Design Control Circuit of Active Power Filter** " examined the students (**Jaafar Mohammed Saleh, Abbas Ali Khamas, Sajjad Hassan Madhboub, Baneen Hassan Hashim**) in its contents and found the project meets the standard for the degree of Bachelor of Science in Electrical Engineering.

Signature:

Name:

Date:

Signature:

Name:

Date:

Signature:

Name:

Date:

Signature:

Name:

Date:

DEDICATION

We believe in the saying, "Every beginning has an end," and here we stand, witnessing the nearing end of our university journey. After enduring years of hard work and dedication, we conclude our graduation research project with all the vigor and enthusiasm we can muster, filled with immense appreciation and gratitude towards everyone who played a role in our journey and extended their help, even if it was minimal.

Praise be to Allah, with love, thanks, and gratitude. We couldn't have achieved this without His grace, so all thanks are to Allah for the beginning and the end.

We dedicate this success to everyone who accompanied us in completing this journey. May you always remain our unwavering support. We also dedicate this research to our beloved family members who taught us values and principles and were a constant source of encouragement and generosity for us.

All thanks be to Allah for enabling us to reach this moment. Praise be to the Lord of all worlds and prayers and peace be upon His noble Prophet.

ACKNOWLEDGEMENT

Praise be to Allah, who guided us to complete this research, and we ask Him to make it beneficial knowledge for everyone.

We extend our deepest gratitude, appreciation, and respect to the supervisor of our research, Dr. Jabbar Rahim Rashid, who spared no effort in guiding and advising us throughout all stages of this work. You have been an invaluable source of inspiration and support, and your insightful feedback and valuable suggestions played a pivotal role in enhancing the quality and objectives of our research.

We greatly value your constant dedication to providing both academic and moral support, and we thank you for your tremendous efforts, which left a significant imprint on our academic journey. You have been a true example of a dedicated and compassionate professor, and we are profoundly grateful for your collaboration and steadfast support throughout this journey.

We pray to Allah to reward you abundantly, bless your efforts, and grant you greater knowledge and distinction.

With utmost appreciation and respect,
Your dedicated students.

ABSTRACT

This research focuses on design control circuit of Active Power Filters (APFs). This filter used to improving the quality of electric power by compensating for reactive power and eliminating harmonics. The performance of single-phase active filters was analyzed using current and voltage control techniques based on Pulse Width Modulation (PWM). The study examined the filter's response in the steady state, the impact of variations in load current with a unity power factor (UPF), and the influence of non-linear loads on filter efficiency. Furthermore, the filter's performance under different load variations was evaluated, considering that the frequency used in all tests was 50Hz, and control was adjusted using a Phase-Locked Loop (PLL) system. The efficiency of the active filter was validated through computer simulations using MATLAB/Simulink software. The simulations included analyzing the system's behavior under various operating conditions, with a focus on reducing Total Harmonic Distortion (THD) and improving the power factor. The results demonstrated that active power filters effectively reduce harmonics and compensate for reactive power, contributing to enhanced stability and efficiency of the electrical grid.

LIST OF FIGURES

<u>Figure</u>		<u>Page</u>
1.1	Voltage source inverter APF	5
1.2	Current source inverter APF	6
1.3	Series active power filter	6
1.4	Shunt active power filter	7
1.5	Single phase loads. (a) Linear Load, (b) Non-linear load	7
1.6	Block diagram of APF	8
2.1	Block diagram of the control circuit for APF (one phase)	18
2.2	(a) and (b) closed loop of the control circuit in a s-domain (one phase)	19
2.3	Filtering characteristics	19
2.4	Response of the closed loop circuit, unit step input with variation of K_p .	20
2.5	(a) PI controller response for current load change at unity power factor. (b) Output of the first multiplier	20
2.6	The flow-chart of Main program. (a) Closed loop control circuit. (b) Flow-chart of program	21
3.1	APF-Block diagram in simulation model	25
3.2	Simulation results for $\theta=0$, $f_s = 50$ Hz, (a) Mains voltage $V_S(t)$ (b) Estimated current $I_a(t)$, (c) Load current $I_l(t)$, (d) Reference current $I_{rh}(t)$.	28

- 3.3 Simulation results for $\theta=90$ lag, $f_s = 50$ Hz, (a) Mains voltage $V_S(t)$ (b) Estimated current $I_a(t)$, (c) Load current $I_l(t)$, (d) Reference current $I_{rh}(t)$. **29**
- 3.4 Simulation results for $\theta=90$ led, $f_s = 50$ Hz, (a) Mains voltage $V_S(t)$, (b) Estimated current $I_a(t)$, (c) Load current $I_l(t)$, (d) Reference current $I_{rh}(t)$. **30**
- 3.5 Simulation results for $\theta=90$ lag, $f_s = 50$ Hz, (a) Mains voltage $V_S(t)$ (b) Estimated current $I_a(t)$, (c) Load current $I_l(t)$, (d) Reference current $I_{rh}(t)$ **31**
- 3.6 Simulation results for $\theta=50$ led, $f_s = 50$ Hz, (a) Mains voltage $V_S(t)$, (b) Estimated current $I_a(t)$, (c) Load current $I_l(t)$, (d) Reference current $I_{rh}(t)$ **32**
- 3.7 Simulation results for Half wave diode rectifier with (R-load) $f_s = 50$ Hz, (a) Mains voltage $V_S(t)$, (b) Estimated current $I_a(t)$, (c) Load current $I_l(t)$, (d) Reference current $I_{rh}(t)$ **33**
- 3.8 Simulation results for Full wave diodes rectifier with (R-load), $f_s = 50$ Hz, (a) Mains voltage $V_S(t)$, (b) Estimated current $I_a(t)$, (c) Load current $I_l(t)$, (d) Reference current $I_{rh}(t)$ **34**
- 3.9 Simulation results for Full wave diodes rectifier with (RL-load), $f_s = 50$ Hz, (a) Mains voltage $V_S(t)$, (b) Estimated current $I_a(t)$, (c) Load current $I_l(t)$, (d) Reference current $I_{rh}(t)$ **35**
- 3.10 Simulation results for Full wave thyristor rectifier with (L-load), $f_s = 50$ Hz, (a) Mains voltage $V_S(t)$, (b) Estimated current $I_a(t)$, (c) Load current $I_l(t)$, (d) Reference current $I_{rh}(t)$ **36**

3.11	Simulation results for pure square wave, $f_s=50$ Hz, (a) Mains voltage $V_S(t)$, (b) Estimated current $I_a(t)$, (c) Load current $I_l(t)$, (d) Reference current $I_{rh}(t)$	37
-------------	---	-----------

LIST OF TABLES

<u>Table</u>		<u>Page</u>
2.1	Routh table for the stability of equation (2.10)	17

LIST OF ABBREVIATIONS

Abbreviation	Definition
TCR	Thyristor-Controlled Reactor
TSC	Thyristor-Switched Capacitor
APF	Active Power Filter
VSI	Voltage Source Inverter
CSI	Current Source Inverter
PWM	Pulse-Width Modulation
PLL	Phase-Locked Loop
P-I	Proportional-integral controller
C.T.	Current transformer
LPF	Low Pass Filter
THD	Total Harmonic Distortion
HIL	Hardware In the Loop
ZVS	Zero-Voltage Switching
DSP	Digital Signal Processors
FPGA	Field-Programmable Gate Arrays
T.F	Transfer function

LIST OF SYMBOLES

Symbol	Description
$i_S(t)$	Mains current
$V_S(t)$	Mains voltage in power circuit
$i_L(t)$	Load current in power circuit
$i_F(t)$	Compensating current
V_{dc}	Voltage of dc side of the VSI
I_{dc}	Current of dc side of the CSI
$V_L(t)$	Load voltage
$i_{rh}(t)$	Reactive and harmonic components of the load current
$i_a(t)$	Active component of the load current
$V_s(t)$	Mains voltage in control circuit
$i_l(t)$	Load current in control circuit
τ	Width of the generated pulses
C	Capacitor of the energy-storage element
L	Inductor of the energy-storage element
$i_r(t)$	Reactive component of the load current
i_a	Peak value of the active components of the load current
i_r	Peak value of the reactive components of the load current
i_{2n}	Peak value of the harmonic components of the load current
i_{2m+1}	Peak value of the odd harmonic components of the load current
ϕ_{2n}	Phase of even harmonic components of the load current
ϕ_{2m+1}	Phase of odd harmonic components of the load current
i_o	Dc component of the load current
K_P	Proportional parameter of P-I controller

K_I	Integral parameter of P-I controller
T_o	Time constant of the LPF
α	Scaling factor of the analogue Multiplier
I_m	Peak value of the load current
θ	Phase shift angle between load voltage and current
ω_o	Cut-off frequency of the LPF
f_s	Frequency of mains voltage
u_o	Initial value of integral part of P-I controller
y_o	Initial value of LPF
y	output of LPF
u	Output of P-I controller
t	Time
x	Output of the first multiplier
f_o	Free running frequency of the VCO
f_c	Capture range frequency of the PLL
ω	Frequency of the load current

TABLE OF CONTENTS

Dedication	I
Acknowledgement	II
Abstract	III
List of Figures	IV
List of Tables	VII
List of Abbreviations	VIII
List of symbols	IX

Chapter One: General introduction

1.1 Introduction	1
1.2 Objectives of the project	5
1.3 Project organization	9

Chapter Two: Basic principle of active power filter

2.1 Introduction	10
2.2 General description	12
2.3 The proposed control strategy	13
2.4 Mathematical model	15
2.5 Simulation results	16
2.5.1 Selection of control circuit parameters	16
2.5.2 The stability test	17
2.6 Conclusion	18

Chapter Three: Implementation and mode of operation

3.1 Introduction	22
3.2 Simulation circuit	25
3.3 Results of simulation	26
3.3.1 Load test	26
3.4 Conclusion	38

Chapter Four: Conclusion and future work

4.1 Summary and conclusions	40
4.2 Suggestions for future work	41
References	42
Appendix A	A1
Appendix B	B1
Appendix C	C1

CHAPTER ONE

GENERAL INTRODUCTION

1.1 Introduction

Nonlinear loads connected to the supply network such as rectifier, inverter and cycloconverter generate high harmonic currents. The harmonic currents have undesirable effects, including additional losses in motors and generating units, overheating in transformers and cables and overloading of capacitors especially when harmonic currents are amplified at resonant frequency. Also, measurement of electricity meters, communication equipment's, electronic control and protection systems may be affected by harmonics noise. The harmonic distortion is not the only drawback of the nonlinear loads. Another disadvantage is the low power factor. Low power factor means excess current in a system, this generates excess copper losses, which results in poor efficiency. For the same power transmitted but at low power factor, the sectional area and size of the conductors are increased to carry more current. Since distortion is unavoidable in a power electronic where will always be some reactive power flow, therefore, the goal of eliminating unwanted harmonics is similar to the goal of eliminating reactive power. A conventional solution to harmonic compensation is the use of passive filter. However, this kind of filter is not adequate due to their inability to compensate for random frequency variations in the current and can produce series and parallel resonance with source impedance. Thereby, this

problem is partially solved with the help of LC passive filters. Various types of static compensators have been proposed and implemented by many researchers, The static compensator, which is based on the thyristor-technology, has been developed and evolved to two basic techniques:

1- Thyristor-Controlled Reactor (TCR).

2- Thyristor-Switched Capacitor (TSC).

These systems usually comprise shunt capacitors and inductors in conjunction with thyristor ON/OFF or phase-controlled switches, to control current in reactive circuit elements (capacitors and inductors). These methods are called variable impedance type reactive power generators. In spite of the many advantages of static compensators circuit, however, various problems still exist. These problems are:

- The thyristors here are used as controlling elements, which operate at low switching frequency.
- The reactive power is provided by large energy storage components such as reactors and capacitors.

This project presents one of the major developments recently applied, namely, the active power filter. This filter has been researched and developed to overcome problems of traditional methods. The next paragraphs introduce the results of an extensive survey on the subject of active power filters. The active power filter (APF) connected to any linear or nonlinear loads is a more interesting solution because it works as current source, that generates the load harmonic currents. Hence, the main only need to supply the fundamental current, avoiding contamination problems. This is the basic operating principle of an APF. The APF uses an inverter and a de

source to generate the required voltage or current waveform. This APF can be operated with two general types of inverter: voltage source inverter (VSI) or current source inverter (CSI) as shown in **Figures 1.1** and **1.2** respectively. The de source of a current inverter consists of an inductor while that of a voltage inverter consists of a capacitor. Also, a separate de source may be connected instead of the inductor or capacitor. Generally, the voltage source inverter is preferred for the active power filter because of its lower losses.. The active power filter can be connected in series or in parallel with the supply network as shown in **Figures 1.3** and **1.4** respectively. The series active power filter works as controllable voltage source and controls the voltage at the load node, allowing excellent regulation characteristics. The shunt passive filter is connected in parallel with the load to eliminate the fifth and seventh harmonics and also helps to partially correct the power factor (12) On the contrary, the shunt active power filter works as a controllable current source and injects the reactive and harmonic currents demanded by the nonlinear load permitting harmonic currents cancellation and power factor improvement without using passive filter. The optimal cancellation of the harmonics will be achieved if the filter. generates the modulating (reference) current identical to the waveform of the present harmonics. The cancellation, entirely, is practically impossible but reduced harmonic distortion to a minimum acceptable level for a given condition can be achieved. It is necessary to transform the reference current into a feasible one by a certain method. The compensating current has been chosen as pulse-width modulation (PWM) current.

The PWM compensating current is obtained from a dc voltage or current source by the inverter circuit. This circuit cannot be made to have the same waveform as the harmonics present in ac lines unless a high modulation frequency is employed. The proper choice of PWM method enables harmonics content of the PWM current to be equal to that of the existing harmonics.

The proposed scheme presented in this work is a shunt active power filter with a voltage source inverter operates as a current-controlled based on pulse-width modulation technique. This filter can compensate for a leading or lagging power factor without sensing and computing the associated reactive power component. Also, it attenuates the amplitude of the harmonic current components generated by nonlinear loads. Conventional control circuits of the APF are generally complex and hard to tune. Also, it may depend on electronic tuned filters and instantaneous power theory, to overcome these disadvantages, the control circuit presented in this work has been proposed and implemented. The new control strategy of the proposed APF generates the reference (modulating) current using accurate and simple processing circuits such as only one load current sensor, subtractor and Phase-locked loop (PLL) estimation circuit. Also, this method is very fast under sudden change in load condition, and it operates successfully in wide range of frequencies. Therefore, this circuit gives better compensation characteristics with any connected load. Finally, the proposed control circuit has been analyzed, simulated and experimentally implemented.

1.2 Objectives of the project

Objectives of this project can be summarized as:

- Explaining the operation principle and analyzing the proposed schemes of single-phase active power filter to determine their behaviors.
- Studying a general control method to achieve compensating characteristics of active power filter connected with any loads and investigating the effect of all parameters on the time response of the circuit by means of computer simulation.
- Testing and investigating experimentally the presented prototypes of the single-phase active power filters for the different loads (linear and nonlinear loads) and different power factors.
- Comparison of the computer simulation results with that obtained experimentally to demonstrate the performance of the proposed filter.

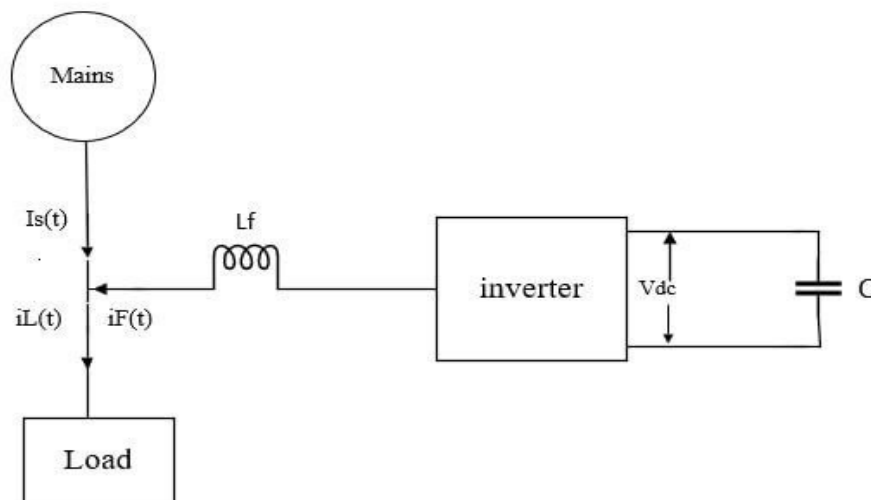


Fig 1.1: Voltage source inverter APF.

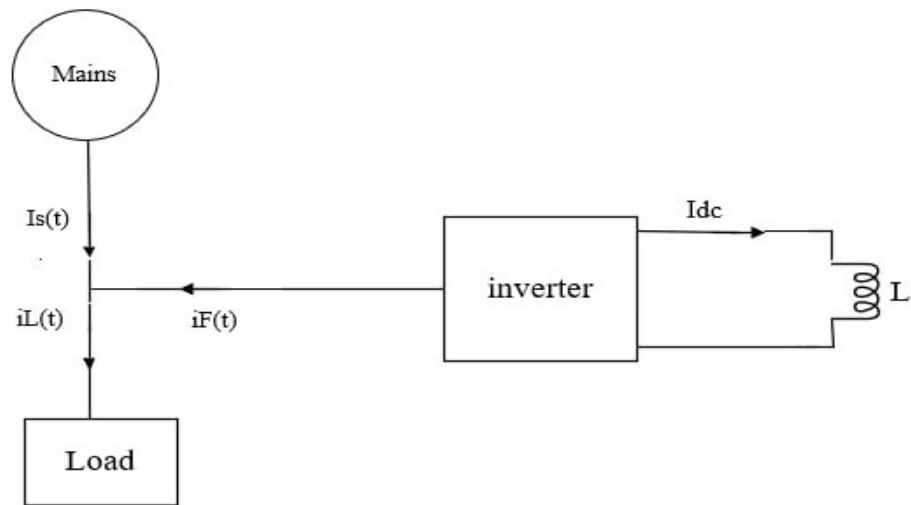


Fig 1.2: Current source inverter APF.

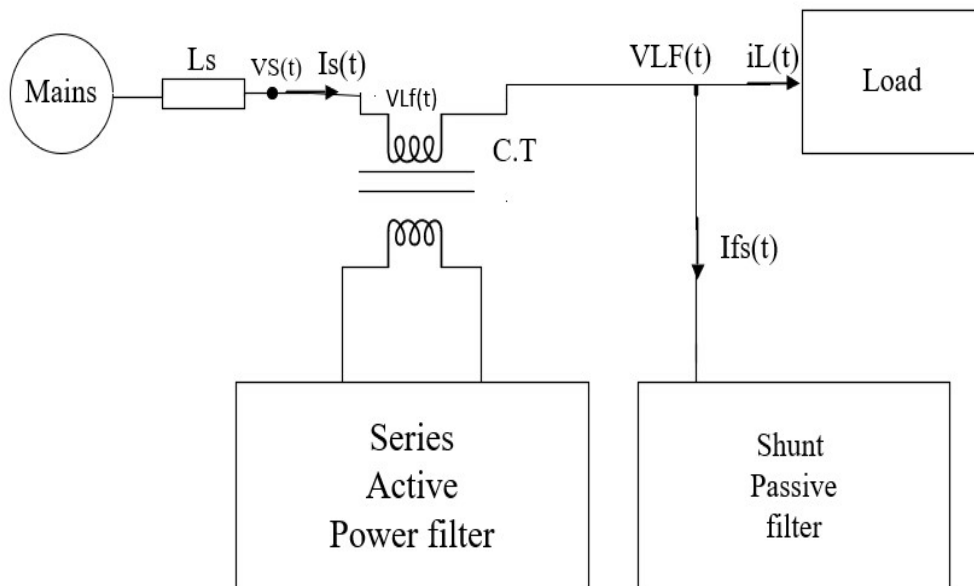


Fig 1.3: Series active power filter.

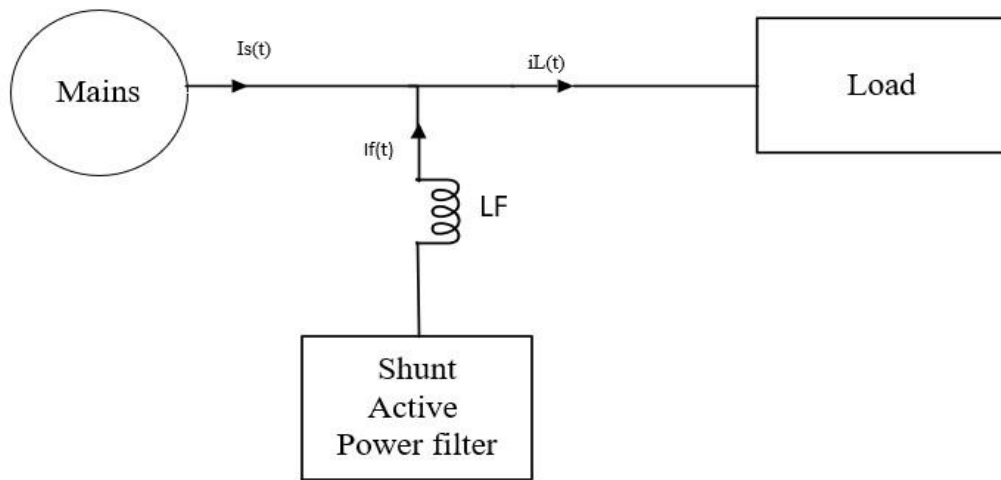


Fig 1.4: Shunt active power filter.

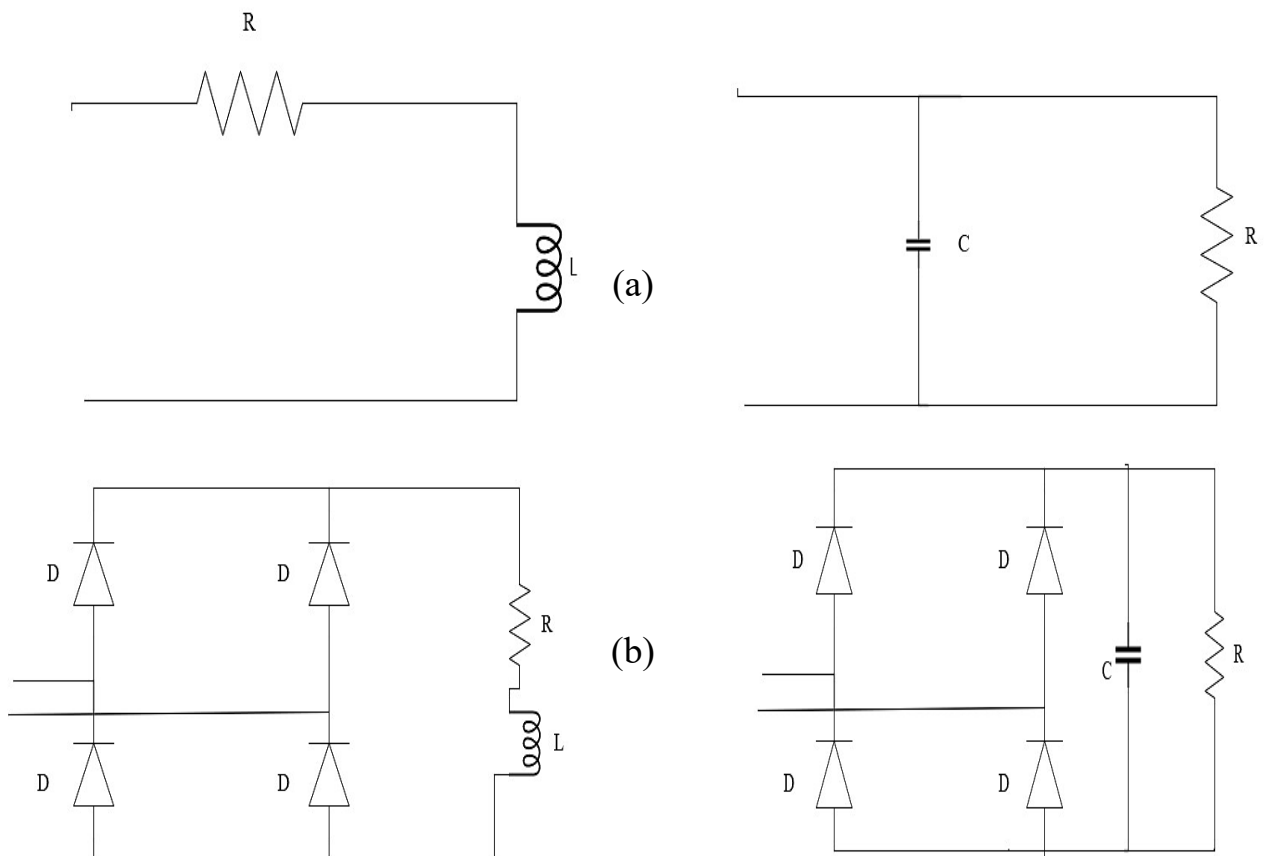


Fig 1.5: Single phase loads. (a) Linear Load, (b) Non-linear load.

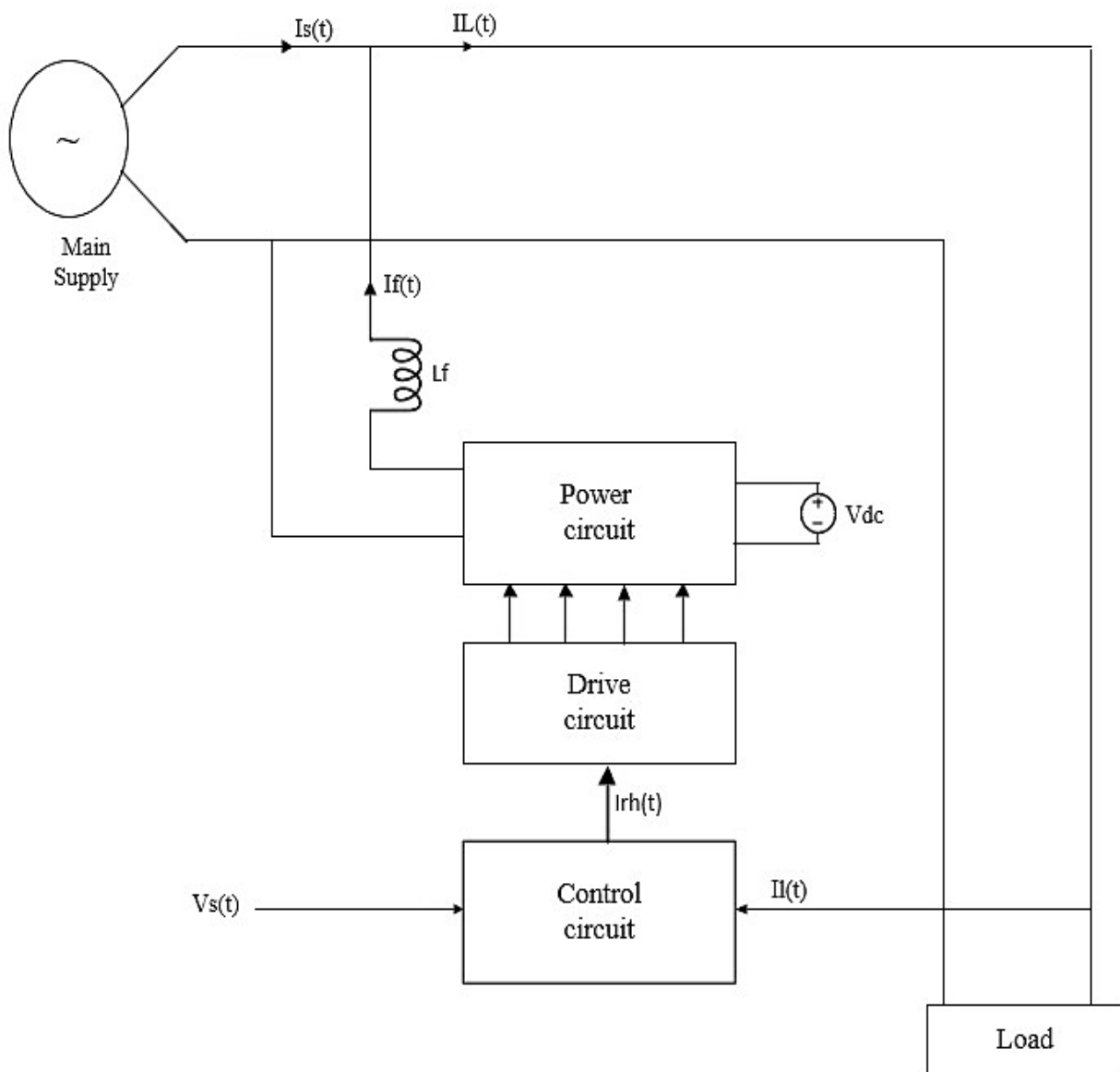


Fig 1.6: Block diagram of APF.

1.3 Project organization

The project contains four chapters:

Chapter one: deals with the theory of reactive power compensation and harmonics cancellation in single phase system. and introduces conventional compensation methods. Also, an introduction to the proposed active power filters has been presented.

Chapter two: gives a complete description of the proposed control circuit including details of the mathematical model and how to select the parameters. Also, the characteristics are verified by computer simulation.

Chapter three: shows clearly the behavior of the control circuit with any load (linear and nonlinear loads) and with different power factors (lagging, unity and leading) in addition to the ability of this circuit in operating at a frequencies of 50Hz.

Chapter four: is developed for discussion and conclusion of the results and overall performance of the system. Future work suggestions are also given in this chapter.

Three appendices are included in this project:

- Appendix (A) 565 PLL
- Appendix (B) Selection of Low pass filter (LPF) elements.
- Appendix (C) Selection of P-1 controller elements.

CHAPTER TWO

Basic Principle Of Active Power Filter

2.1 Introduction

The heart of the active power filter in the control circuit is not only crucial because this circuit implements the APF compensation characteristics, but also because it is responsible for generating the current. Innovations in modern approaches of active power filters are presenting novel techniques to generate this current. These techniques have made remarkable progress in achieving desirable technical features, such as fast response time, ease of integration, and commercial success due to their acceptable cost.

The conventional control methods of the active power filter used to obtain the required reference current are based on electronic filters and instantaneous power theory. Electronic filters, usually of the band-pass filter type, have the drawback that a small change in the mains frequency may cause a significant phase shift at the output. Therefore, to overcome this problem, precision components and frequency adjustments have been used, but this would be valid only for the operating frequency and would not compensate for changes due to component aging and temperature. On the other hand, the instantaneous power theory usually requires four to six high-precision analog multipliers and dividers per phase to implement the

transformations. Thus, this circuit becomes complex and sensitive to Component parameter variations.

In this work, a new control strategy for single-phase active power filters is presented and analyzed. This approach is quite different in principle from the conventional control strategies, providing better compensation characteristics. The proposed method offers the following advantages:

- The presented technique is simple than the instantaneous power theory-based design because this method has only two multipliers per phase and only one current sensor.
- This approach is better than the compensators that are based on the concept of electronic filters because they can operate properly in the continuous change of frequencies from 40 to 60 Hz.
- The adopted method responds very fast under sudden changes in load conditions and reaches its steady state in about two cycles of the fundamental frequency when there is a proper selection of parameters.

The scope of investigation of this chapter includes general description well as the principle of operation and performance of the proposed control circuit. other areas of investigation include the design of this circuit to produce the required characteristics. Then computer simulations are verified.

2.2 General description

The load current formed by the power factor and harmonics and is made up of the following four terms:

$$i_l(t) = I_o + i_a(t) + i_r(t) + i_h(t) \quad (2.1)$$

Where:

I_o : Dc component

i_a : Active component

i_r : Reactive component

i_h : Odd and even harmonics component

Equation (2.1) can be expanded as shown in equation (2.2) to show more details about the load current, i.e.

$$I_l(T) = I_o + I_a \cos(\omega t) + I_r \sin(\omega t) + \sum_{n=1}^{\infty} I_{2n} \cos(2n\omega t + \varphi_{2n}) + \sum_{m=1}^{\infty} I_{2m+1} \cos(2m+1)\omega t + \varphi_{2m+1} \quad (2.2)$$

The first term in equation (2.2) which represents the de component is usually small or it does not exist at all. The only component that the mains should supply is the active current, which is really the second term whereas the third term ($I_r \sin \omega t$) stands for the reactive current. The other two final terms comprise the even and odd harmonic components in the load current

respectively. If the active power filter supplies the required dc, reactive and harmonic currents to the load, then the mains need only to supply the active current. The APF current is easily obtained by subtracting the active current $i(t)$ from the measured load current $i(t)$ as follows:

$$i_{rh}(t) = i_l(t) - i_a(t) = i_l(t) - i_a \cos(\omega t) \quad (2.3)$$

Where in $i(t)$ clearly enough, it represents all the components in the load current except the active component. From equation (2.3), it can be noticed easily that i_a is the magnitude of in-phase current (which needs to be estimated) and $(\cos \omega t)$ is the sinusoid in-phase with the mains voltage. To achieve the experimental realization of equation (2.3), two sensors are needed, the first one is to detect the load current and the other to sense the mains voltage.

2.3 The proposed control strategy

The block diagram of the proposed control circuit for active power filter (one phase) is shown in **Figure 2.1**. Multiplying the load current given in equation (2.2) by $(\cos \omega t)$ results in equation (2.4):

$$\begin{aligned} i_l(t) \cdot \cos(\omega t) &= I_o \cos(\omega t) + \frac{I_a}{2} + \frac{I_a}{2} \cos(\omega t) + \frac{I_r}{2} \sin(2\omega t) \\ &+ \sum_{n=1}^{\infty} \frac{I_{2n}}{2} [\cos((2n+1)\omega t + \phi_{2n}) + \cos((2n-1)\omega t + \phi_{2n})] \\ &+ \sum_{m=1}^{\infty} \frac{I_{2m+1}}{2} [\cos((2m+2)\omega t + \phi_{2m+1}) + \cos((2m-2)\omega t + \phi_{2m})] \quad (2.4) \end{aligned}$$

In equation (2.4), the term $\frac{I_a}{2}$, is proportional with the magnitude of the active component and it can be extracted by using the control circuit shown in **Figure 2.1**. In this circuit, the cut-off frequency of the low pass filter is chosen below the lowest frequency component of the line current. Therefore, all frequencies that are equal to or greater than (ω) will be attenuated. The complete attenuation of components (having frequencies $\geq \omega$) gives a good estimation of the active current amplitude (I_a). Then, the estimated amplitude (I_a) is multiplied by a unity sinusoid in-phase with the mains voltage to obtain an estimation of the active current $I_a(t)$. Being estimated, the active current is fed with the measured load current to summing node to generate the required reactive and harmonics current which is called the reference current. To analyze the circuit shown in **Figure 2.1**, assume it has reached a steady state condition and the estimated active current $I_a(t)$ is an accurate representation of in-phase component in the load current.

After subtraction, the output of the summing node will be as stated in equation (2.3). Then, by definition and agreement $I_a(t)$ should not have an active component because it is subtracted from the load current $i(t)$. After multiplication with $(\cos \omega t)$, no dc component will be present. as can be observed in equation (2.4) by letting $I_a = 0$. This means that the ΔI_a , as shown in **Figure 2.1** will be zero, which will keep the output of the P-1 controller I_a , constant. Finally, the output of the P-I controller will exactly correspond to the magnitude of the active current $I_a(t)$ if the load current is not changed. In **Figure 2.1**, The method used to implement the line voltage in-phase sinusoid generator block, consists of a PLL circuit. The PLL technique has a unique phase tracking of the line voltage over operating frequency range (40-60) Hz. Also, this circuit blocks efficiently the distortion

in the line voltage and generates a clean sinusoid even if the input is a square wave.

2.4 Mathematical model

The control circuit in the previous section can be represented in s-domain as shown in **Figure 2.2-b**. The open loop transfer gain of this circuit is:

$$G(S) = \frac{a^2(K_P S + K_I)}{S(T_O S + 1)} \quad (2.5)$$

The closed loop transfer function of the control circuit can be derived as follows:

$$I_{rh}(S) = I_l(S) - I_a(S) \quad (2.6)$$

And

$$I_a(S) = G(S) - I_{rh}(S) \quad (2.7)$$

Using equations (3.6) and (3.7), the relationship between $I_a(S)$ and $I_l(S)$ can be shown to be:

$$\frac{I_a(S)}{I_l(S)} = \frac{\frac{\alpha^2 K_p}{T_O} S + \frac{\alpha^2 K_I}{T_O}}{S^2 + \frac{1}{T_O} (\alpha^2 K_p + 1) S + \frac{\alpha^2 K_I}{T_O}} \quad (2.8)$$

2.5 Simulation results

This section investigates the effect of circuit parameters on the response of the system. These parameters are determined by the iterative computer simulation. The values obtained from this test enable the designer to select the best possible response of the circuit. Further, this section studies the performance, accuracy and stability of the designed control circuit. Also, the simulated results of linear and nonlinear load tests will be introduced.

2.5.1 Selection of control circuit parameters

The parameters of the low pass filter, P-I controller and analogue multiplier have been selected to give a good compromise between output overshoot and settling time. Choosing the scaling factor of the analog multiplier (a) as IV/V and the time constant of the low-pass filter (t) as 0.094 sec. (i.e. the cut-off frequency of 10 Hz) gives good attenuation for frequencies equal to or greater than the mains frequency. The filtering characteristics of the low pass filter for the chosen parameters is shown in **Figure 2.3**. An improvement in the response of the closed loop circuit has been obtained by the proper choice of the P-I controller coefficients. These coefficients are determined by iterative computer simulations of the controller response for different values of K_e and K . The effects of the proportional parameter K_p , and integral parameter K_i , of the P-I controller on the response of the control circuit are illustrated in the curves of **Figures 2.4** and **2.5** respectively. From **Figure 2.4**, it is clear that optimal response of the system is obtained with $K_p = 35$. Also, the effect of the another coefficient K_i on the response is investigated using **Figure 2.5**, where good stability of the system is obtained with $K_i = 400$ for the considered specifications, Finally,

the consequence of electing the optimal values for K_p and K as showed in **Figure 2.6**, Where the response of the P-I controller reaches its steady-state value in about two cycles without any overshoot in the current amplitude.

2.5.2 The stability test

Using the selected values for a , T_o , K_p and K , in equation (2.8) yields equation (2.9):

$$\frac{I_a(S)}{I_l(S)} = \frac{372.978S+4255.32}{S^2+382.978S+4255.32} \quad (2.9)$$

The Routh and Hurwitz criteria has been used to investigate stability of the analyzed system [36]. The characteristic equation of the closed loop transfer function is:

$$S^2 + 382.978S + 4255.32 = 0 \quad (2.10)$$

Using this characteristic equation, Routh table for stability is listed below:

Table 2.1: Routh table for the stability of equation (2.10)

S^2	1	4255.32
S^1	382.978	0
S^0	4255.32	0

For stability reasons, the first column terms in **Table (2.1)** must not change in sign, therefore the presented system is stable. Also, since the equation (2.10) has only positive coefficients, then it is always stable.

2.6 Conclusion

The control circuit represents a major part of APF since the performance, complexity and cost of the filter depend mainly on its control circuit. In addition to the main task of the control circuit in the reactive power compensation and harmonic cancellation, it must respond as quickly as possible for any change in its inputs without causing a serious overshoot in the circuit currents or voltages.

In this chapter, the implemented control circuit has been investigated, by simulations, for different trouble load conditions. The simulation results show that this control circuit can perform its job accurately and efficiently under all the assumed conditions such as the sudden change in the magnitude and phase of the load current, change in the operating frequency of the power system and also under the condition of linear or nonlinear load.

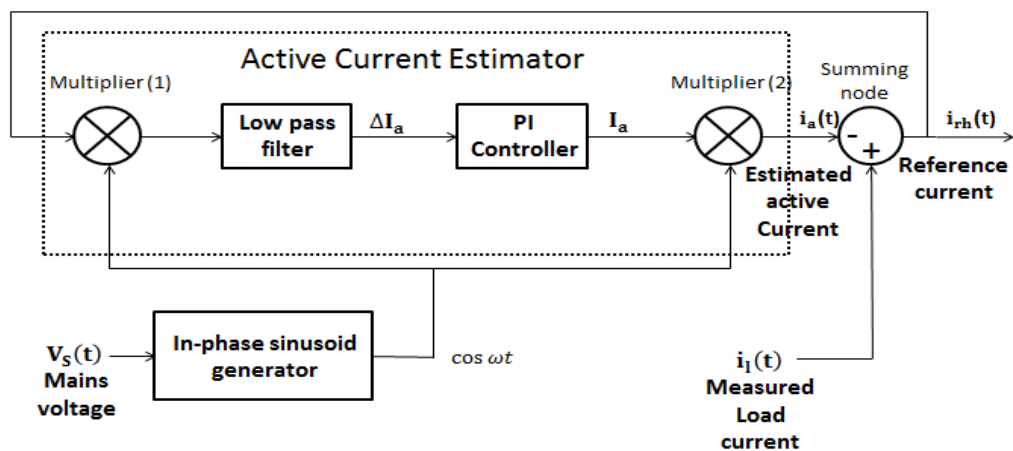
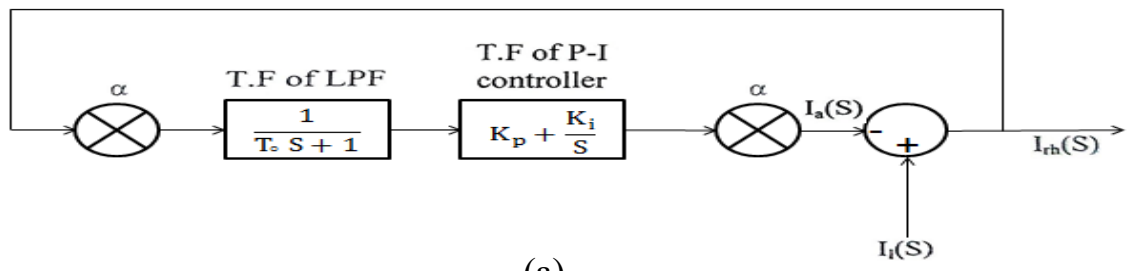
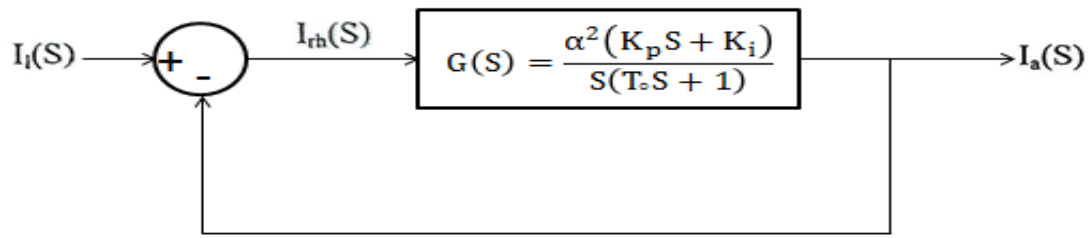


Fig 2.1: Block diagram of the control circuit for APF (one phase).



(a)



(b)

Fig 2.2: (a) and (b) closed loop of the control circuit in a s-domain (one phase).

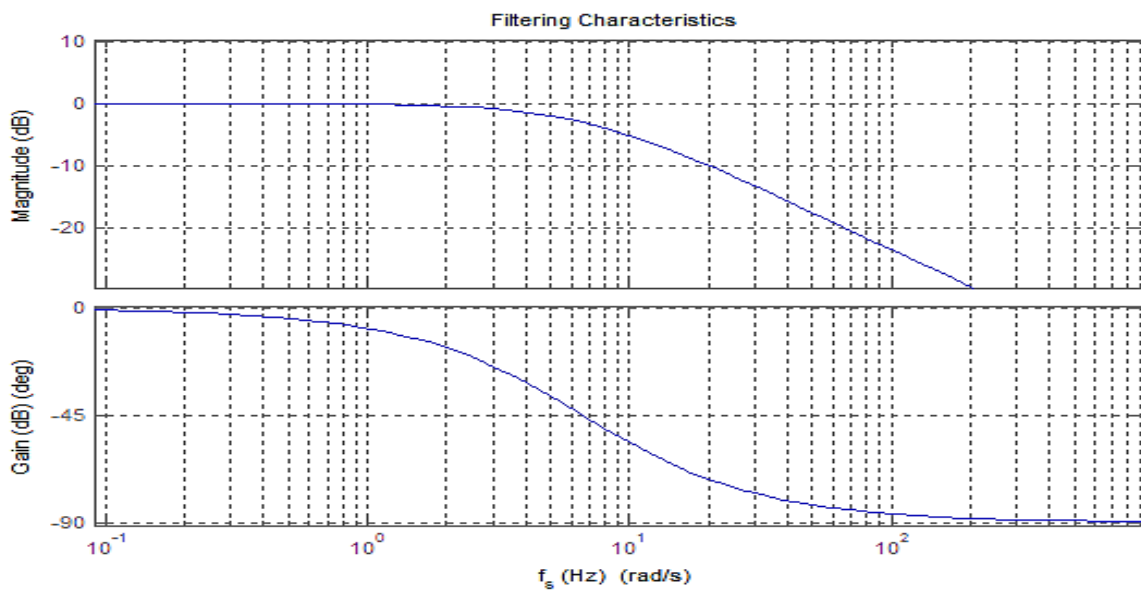


Fig 2.3: Filtering characteristics.

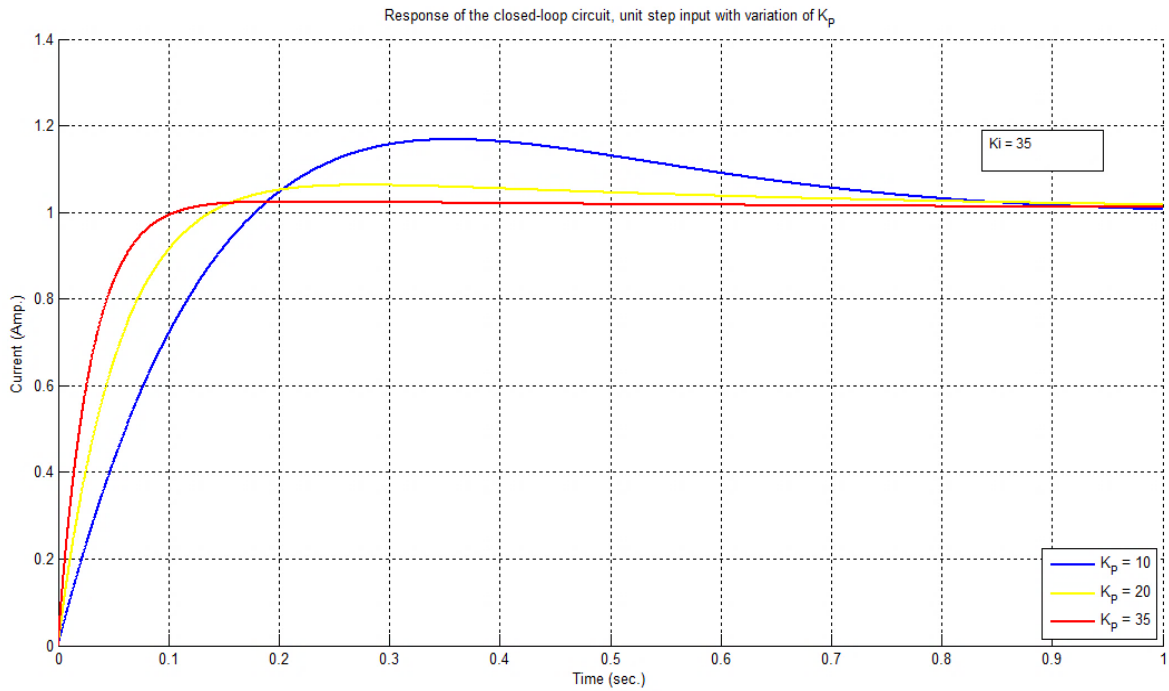


Fig 2.4: Response of the closed loop circuit, unit step input with variation of K_p .

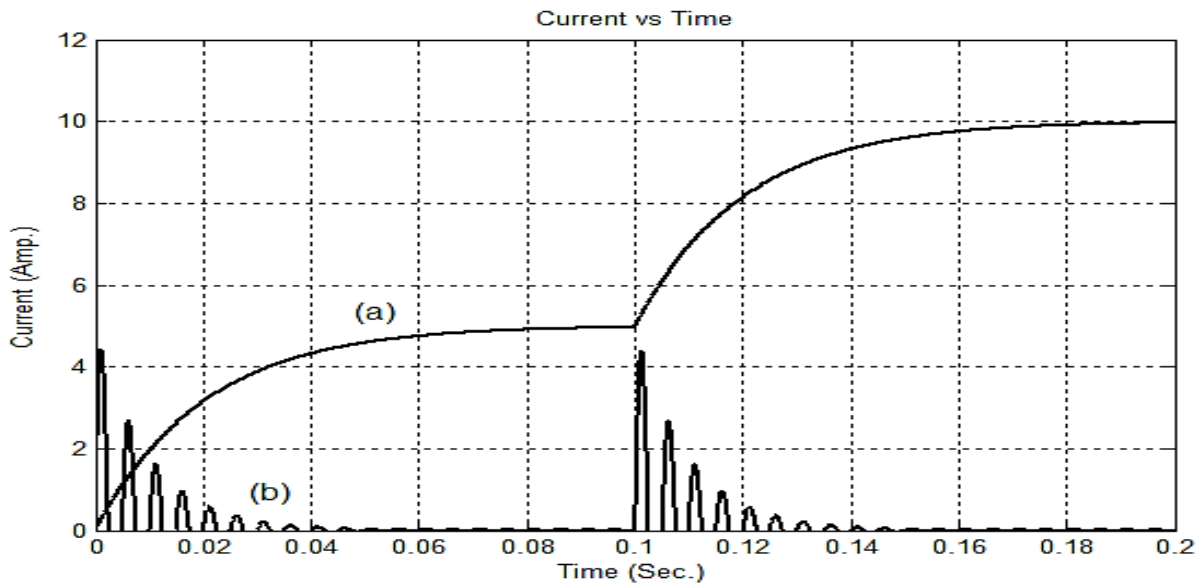


Fig 2.5: (a) PI controller response for current load change at unity power factor. (b) Output of the first multiplier.

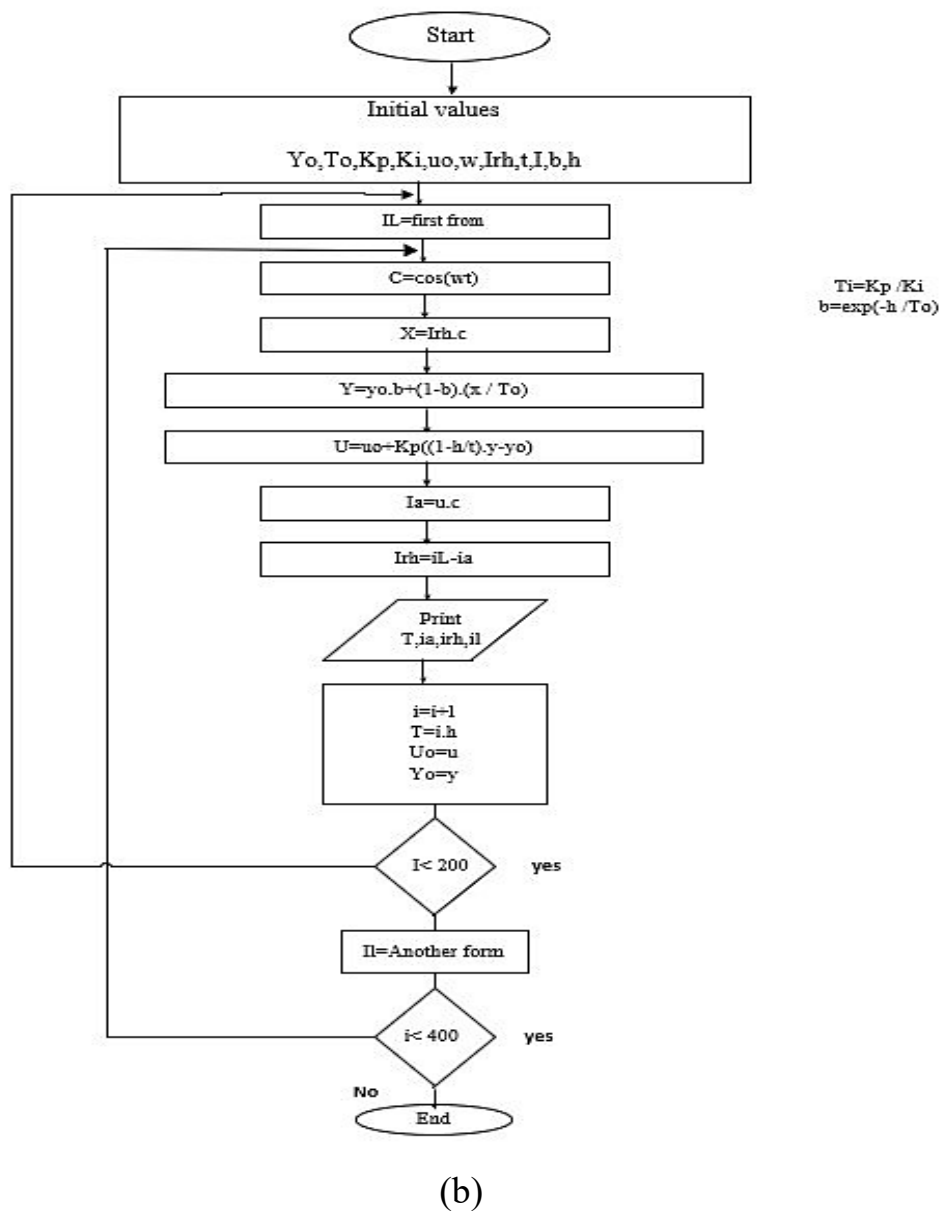
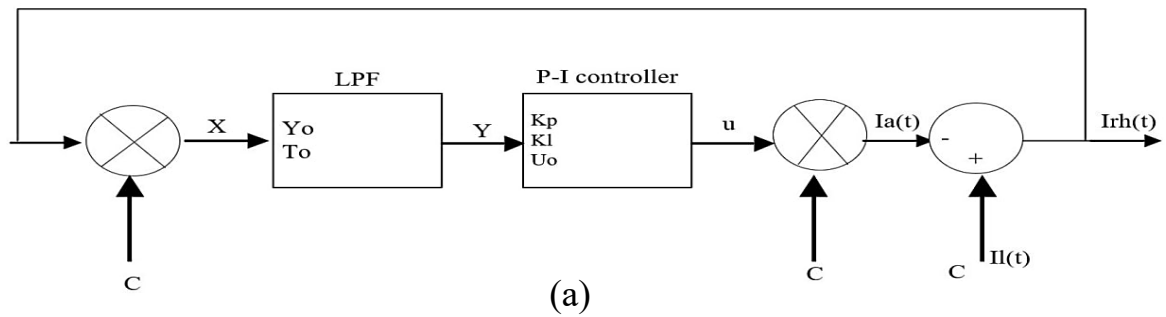


Fig 2.6: The flow-chart of Main program. (a) Closed loop control circuit.
(b) Flow-chart of program.

CHAPTER THREE

Simulation Model Of Control Circuit

3.1 Introduction

This chapter presents a comprehensive analysis of the results obtained from our research on enhancing power quality using an Active Power Filter (APF) based on an estimated current method. In **Figure 2.7** The study was initiated to address the growing challenges posed by harmonic distortions in modern electrical systems, particularly those introduced by nonlinear loads. In order to provide a robust solution, our research focused on developing an approach that not only reduces Total Harmonic Distortion (THD) but also enhances the dynamic stability of the power system. In this introduction, we outline the experimental framework, describe the simulation environment, and summarize the key findings that emerge from our analysis. The research methodology is anchored in advanced simulation techniques executed within MATLAB/Simulink, in **Figure 3.1** where a series of experiments were conducted under varying operational conditions. The core objective was to evaluate how well the estimated current method performs in real-time harmonic mitigation when integrated into an APF system. Unlike conventional techniques-such as those based on instantaneous reactive power theory or synchronous reference frame control, the estimated current method was designed to predict and counteract

harmonic currents more effectively, thereby achieving smoother waveform outputs and faster response times. This approach is particularly significant in scenarios where rapid load variations and transient conditions are prevalent. In setting up the experiments, multiple simulation scenarios were crafted to mirror realistic operating conditions of power systems.

These scenarios included steady-state operations, sudden load changes, and transient disturbances. Each scenario was meticulously analyzed to assess how the estimated current method influences key performance metrics. The simulations provided valuable insights into the extent of harmonic reduction, the improvement in current waveform quality, and the overall robustness of the APF. Detailed waveform analyses and statistical measurements, such as the quantification of THD and the evaluation of response time, formed the backbone of our results. Such rigorous testing enabled us to validate the efficacy of the proposed method and identify areas where further optimization might be necessary. A pivotal aspect of our research was the comparative evaluation of the estimated current method against traditional filtering approaches. By benchmarking our method with conventional techniques, we were able to highlight both the strengths and the potential limitations inherent in our approach. The comparative study revealed that the estimated current method not only delivers superior performance in terms of harmonic suppression but also exhibit enhanced adaptability to rapidly changing load conditions. The resulting improvement in the quality of the source current waveform underscores the potential of this method as a viable solution for modern power systems that demand high levels of power quality and reliability. Another important facet of the study was the examination of various system parameters and their impact on APF performance. Parameters such as the

switching frequency, DC-link voltage, and filter inductance were systematically varied to determine their optimal ranges. This sensitivity analysis provided deeper insights into how these factors influence the efficiency of harmonic mitigation.

For instance, it was observed that higher switching frequencies generally lead to better performance, though at the cost of increased switching losses. Similarly, the DC-link voltage and filter inductance were found to play critical roles in shaping the overall response of the APF. Such findings are crucial as they guide the design and tuning of APF systems for practical applications, ensuring that the method can be adapted to meet diverse operational requirements. The analysis also delves into the dynamic behavior of the APF when subjected to transient disturbances. Transient events in power systems can cause significant deviations in voltage and current profiles, which in turn affect the stability and efficiency of the network. Our results indicate that the estimated current method demonstrates a notable resilience in the face of such disturbances, quickly stabilizing the system and maintaining a lower THD. This resilience is a critical advantage in modern power systems, where the prevalence of fast-changing load profiles and intermittent renewable energy sources demands a more agile filtering solution. Moreover, the study highlights several practical implications of implementing the estimated current method in real-world scenarios. The enhanced harmonic suppression capability not only contributes to improved system efficiency but also extends the operational lifespan of electrical equipment by reducing stress on components. In industrial and commercial settings, where power quality directly impacts productivity and safety, such improvements are highly valuable. The research outcomes therefore offer promising avenues for further

development and commercialization of APF systems based on advanced current estimation techniques. Despite the promising results, the research also identified certain challenges and limitations that warrant further investigation.

One notable challenge is the complexity involved in accurately estimating the current under highly dynamic conditions. This challenge necessitates a precise calibration of the APF control parameters and may require the integration of additional adaptive algorithms to maintain optimal performance. Additionally, the computational overhead associated with real-time estimation must be balanced against the benefits in harmonic reduction. Addressing these challenges is a critical next step, and future work could explore the incorporation of machine learning techniques to further refine the estimation process and reduce computational demands.

3.2 Simulation circuit

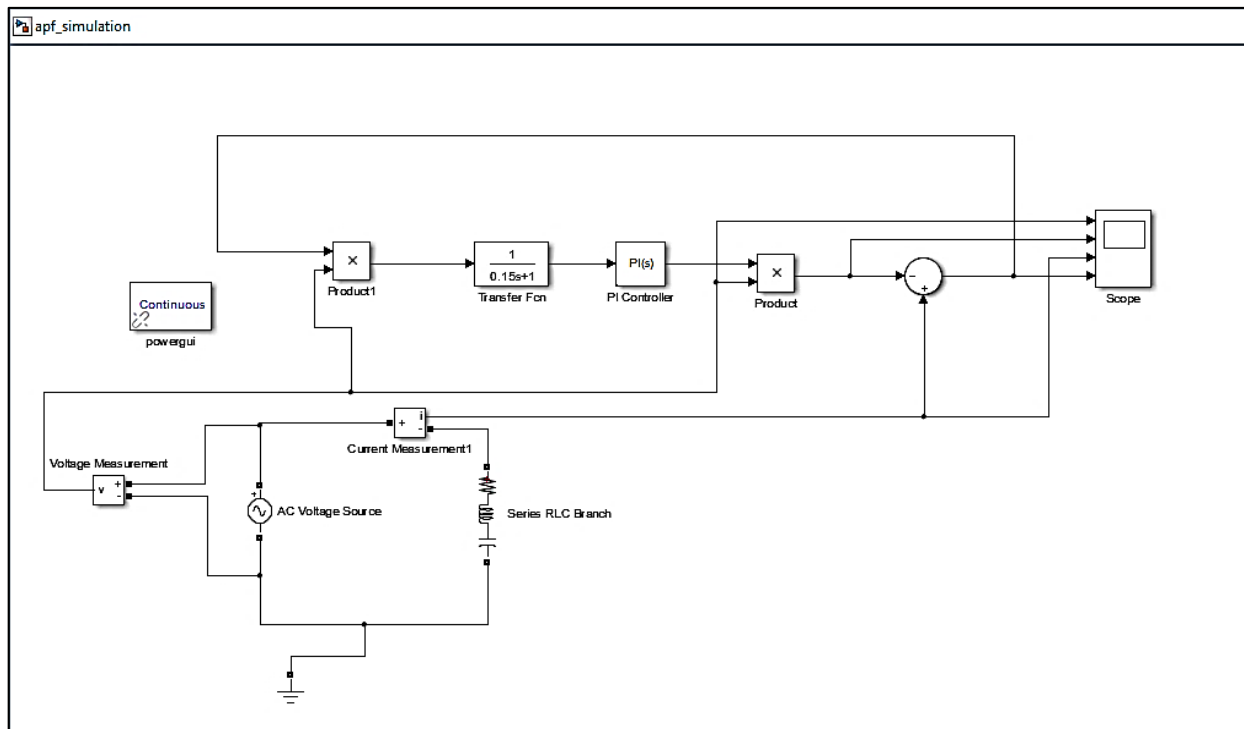


Fig 3.1: APF-Block diagram in simulation model.

3.3 Results of Simulation

3.3.1 Load test

In this section, the computer simulations were run with different types and magnitudes of the load current to check the performance of the control circuit. Simulation results show that excellent harmonic cancellation and reactive power compensation can be achieved by the designed control circuit for all the simulated cases. **Figure 2.7** shows the flow chart that describes the processes performed to simulate the operation of the control circuit for the different study cases. This control circuit has been subjected to the following simulation conditions:

(a) Change in the magnitude of a UPF load current.

Figure 3.2 shows the response of the control circuit for a change in the magnitude of the current. As it can be seen from this figure, the response of the circuit reaches its steady value in about two cycles which is given acceptable time in power system control.

For a load with unity power factor, a change in its magnitude will produce momentary harmonic current and distortion in the active current as illustrated in **Figures 3.2-b** and **3.2-d**. Also, from this figure one can conclude that the active power filter will not inject any current in power system for unity power factor and all the load current will be supplied by the mains.

(b) Change in the magnitude of the load current with different power factors.

In this case, the current takes the following form:

$$I_l(t) = I_m \cos(\omega t + \theta) \quad (3.1)$$

The control circuit has been investigated for a change in the load current for different power factors. **Figure 3.3** illustrates the key waveforms for a load current displacement of 90 lagging whereas **Figure 3.4** shows them for 90 leading. Greater phase displacement effect on the control circuit response is illustrated in **Figures 3.5** and **3.6**.

The simulation results for the different phase displacements considered above show that the control circuit performs its function efficiently and the reactive current supplied by the active filter will be increased according to the reactive component of the load current.

(c) Nonlinear load test.

Now, the load current is represented as a waveform contains a fundamental plus 5,7 and Ninth harmonics as shown in **Figures 3.8** and **3.9**. Simulations of load current with high order of harmonics are illustrated in **Figures 3.10** and **3.11**. The simulation results for the non-linear load show that these loads are associated with harmonics and reactive power generation by the active power filter. Also, half wave rectifier load requires that active power filters supply the component of the load current as shown in **Figure 3.7**.

The response of the control circuit for their loads has proved its effectiveness and validity for the harmonic and reactive power compensation.

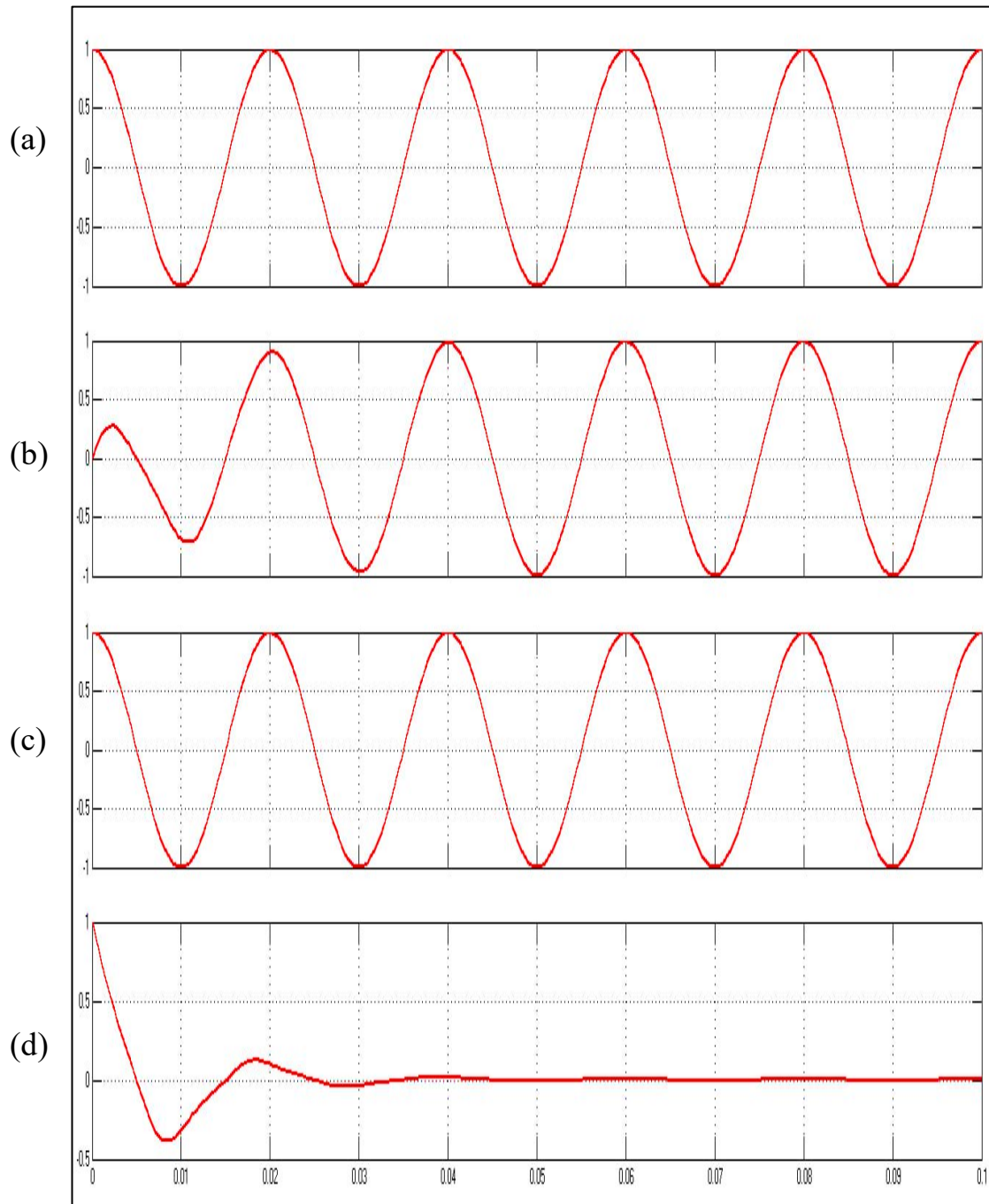


Fig 3.2: Simulation results for $\theta=0$, $f_s=50$ Hz, (a) Mains voltage $V_S(t)$, (b) Estimated current $I_a(t)$, (c) Load current $I_1(t)$, (d) Reference current $I_{rh}(t)$.

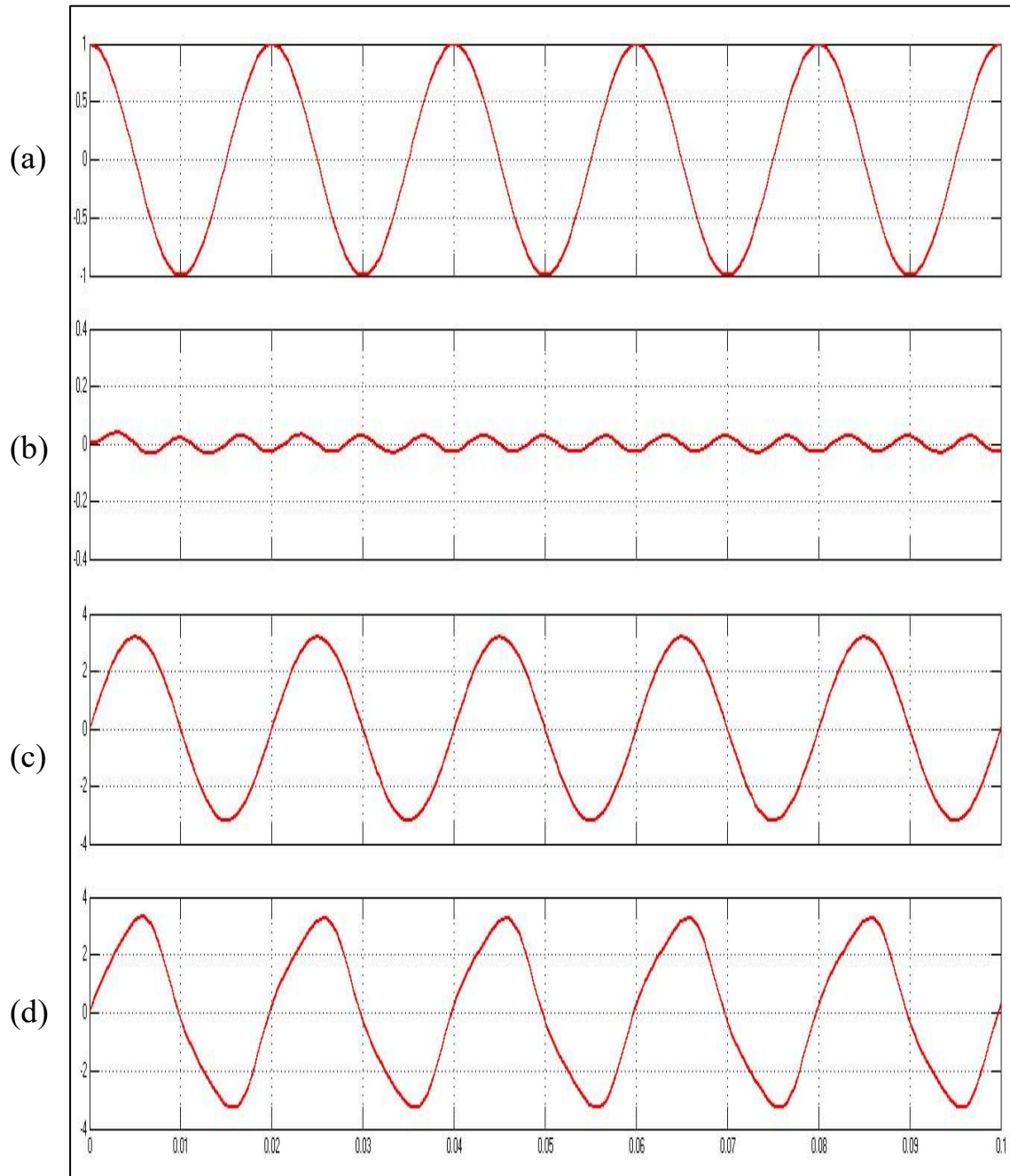


Fig 3.3: Simulation results for $\theta=90$ lag, $f_s=50$ Hz, (a) Mains voltage $V_s(t)$, (b) Estimated current $I_a(t)$, (c) Load current $I_l(t)$, (d) Reference current $I_{rh}(t)$.

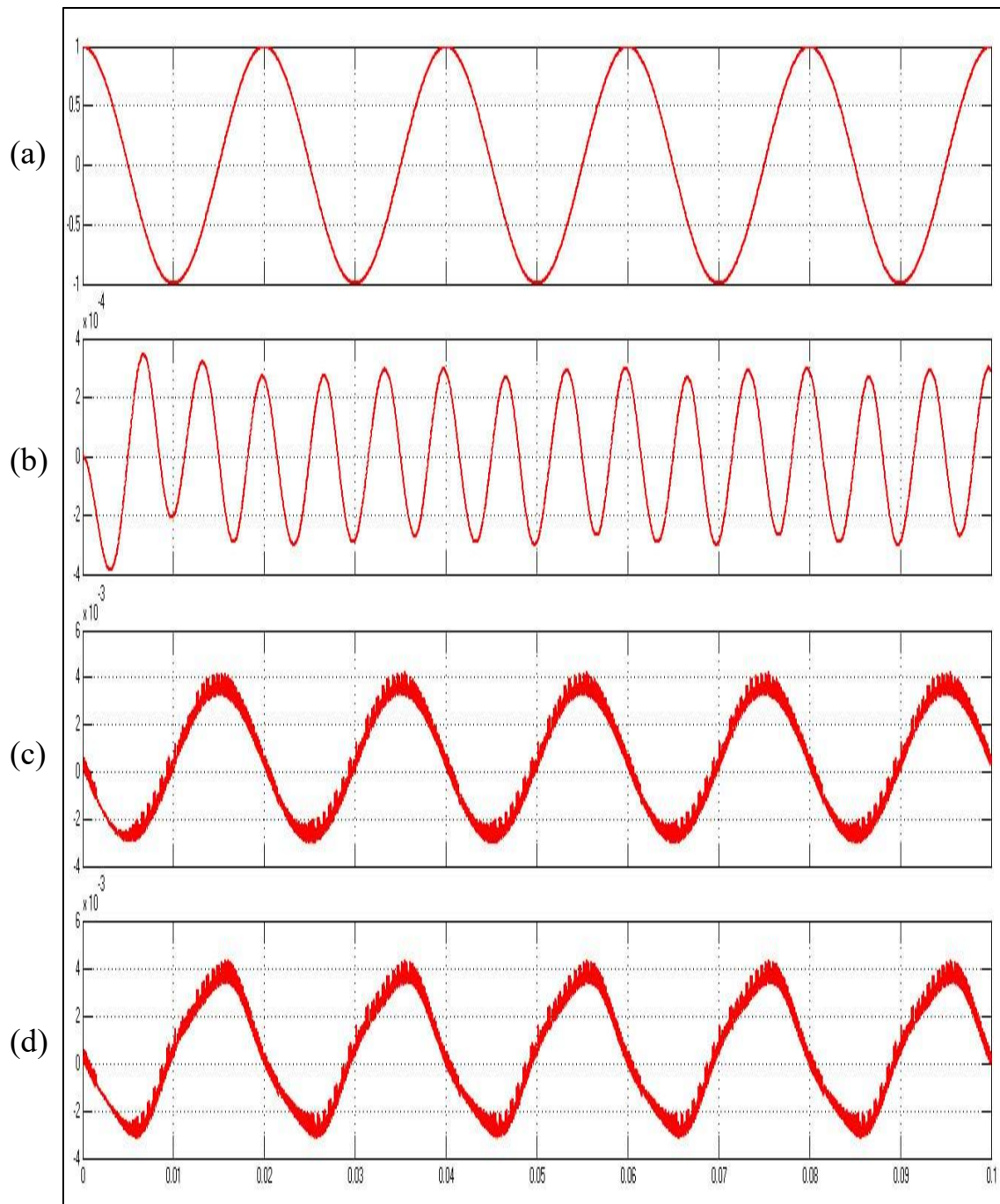


Fig 3.4: Simulation results for $\theta=90$ led, $f_s=50$ Hz, (a) Mains voltage $V_S(t)$ (b) Estimated current $I_a(t)$, (c) Load current $I_1(t)$, (d) Reference current $I_{rh}(t)$.

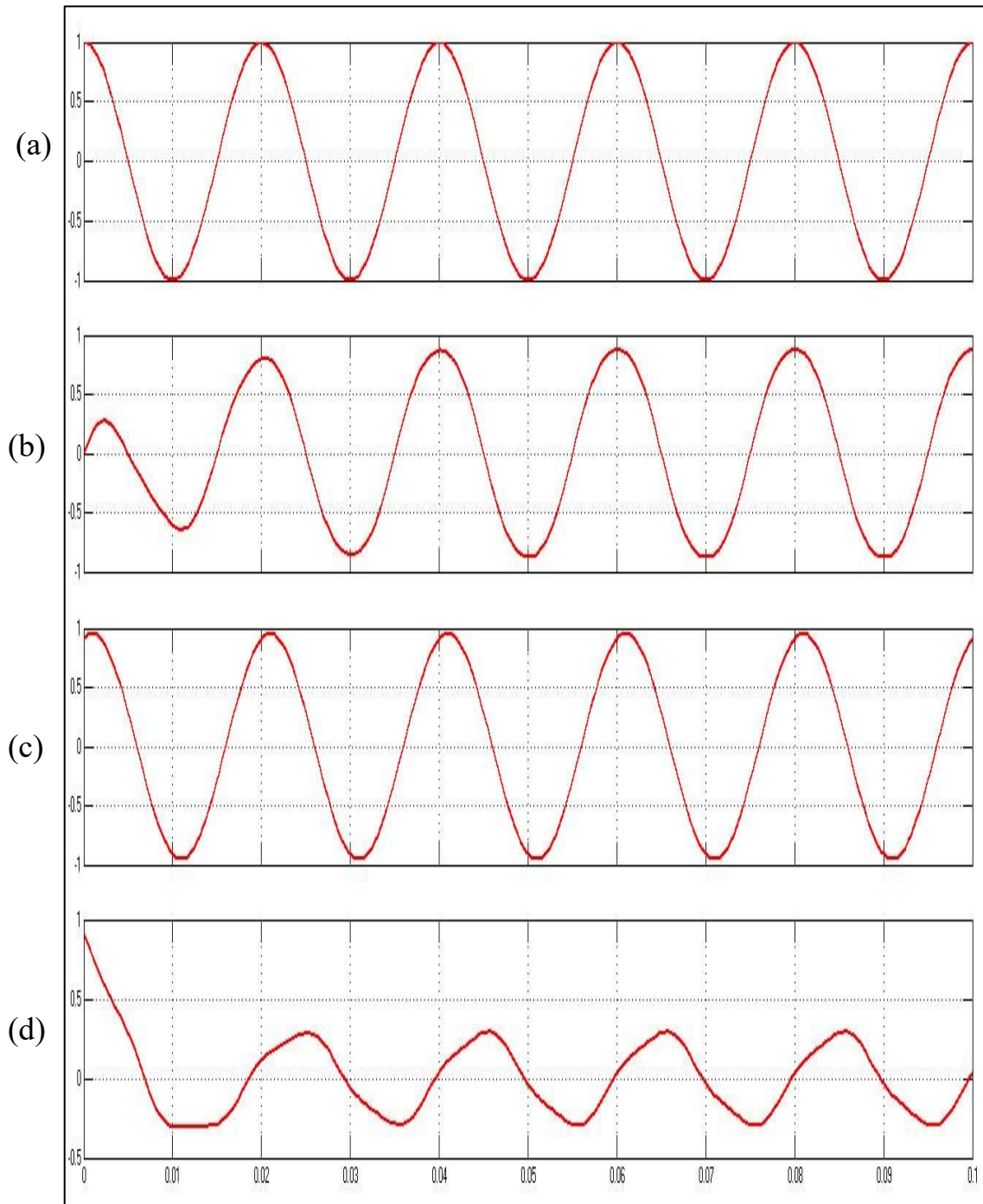


Fig 3.5: Simulation results for $\theta=90$ Lag, $f_s = 50$ Hz, (a) Mains voltage $V_S(t)$ (b) Estimated current $I_a(t)$, (c) Load current $I_1(t)$, (d) Reference current $I_{rh}(t)$.

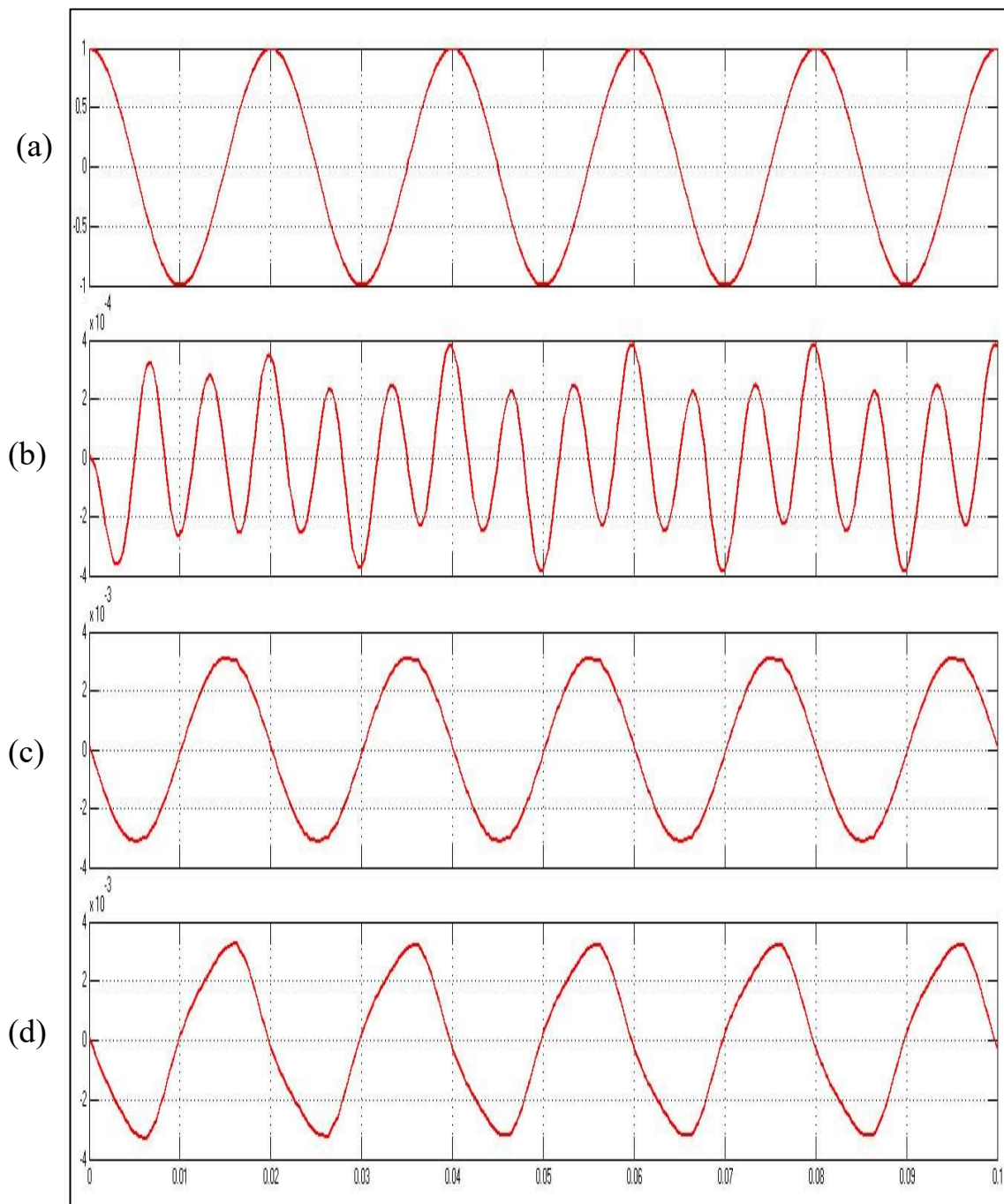


Fig 3.6: Simulation results for $\theta=50$ led, $f_s=50$ Hz, (a) Mains voltage $V_s(t)$ (b) Estimated current $I_a(t)$, (c) Load current $I_l(t)$, (d) Reference current $I_{rh}(t)$.

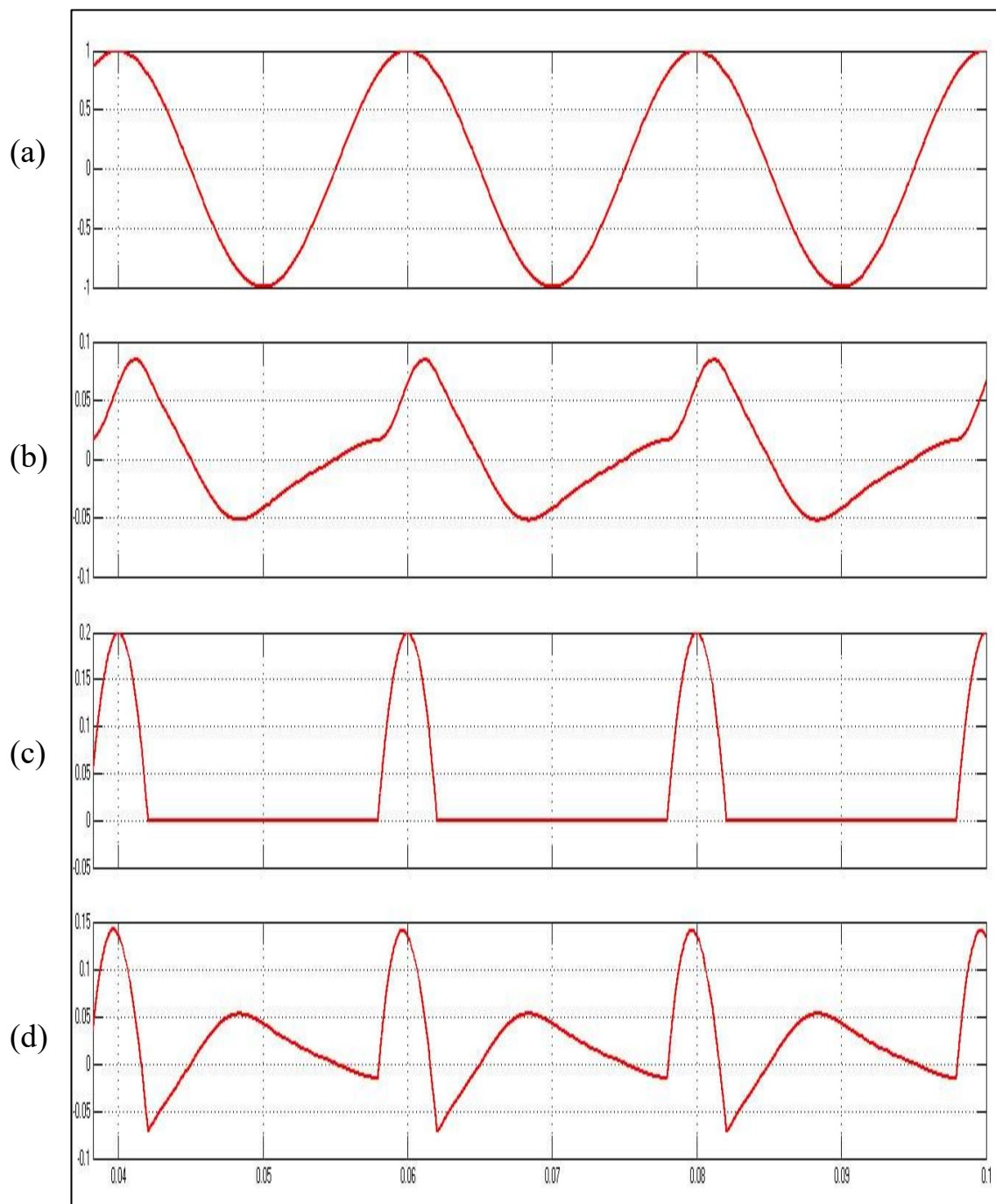


Fig 3.7: Simulation results for half wave diode rectifier with (R-load) $f_s=50$ Hz, (a) Mains voltage $V_s(t)$, (b) Estimated current $I_a(t)$, (c) Load current $I_l(t)$, (d) Reference current $I_{rh}(t)$.

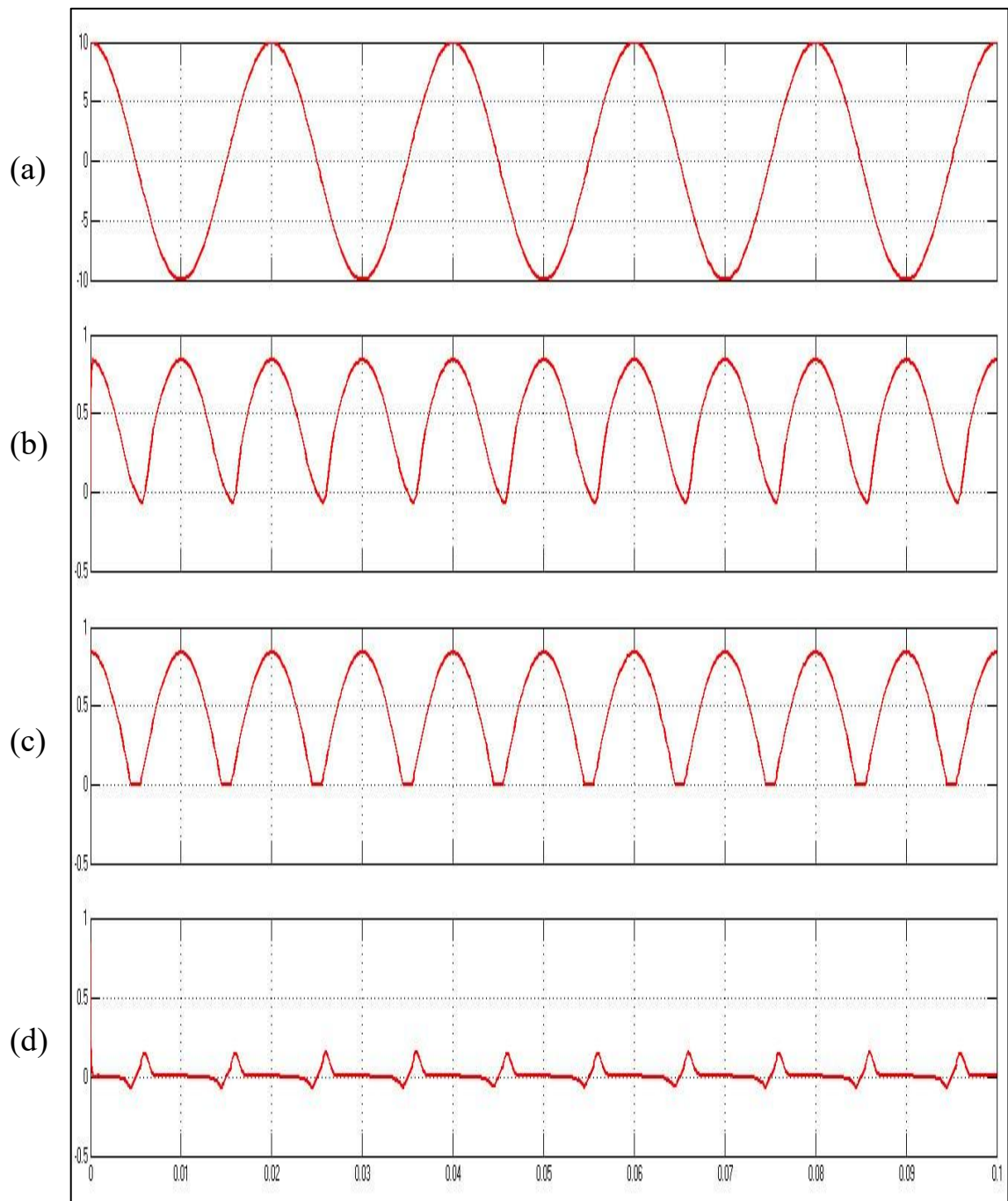


Fig 3.8: Simulation results for Full wave diodes rectifier with (R-load), $f_s = 50$ Hz, (a) Mains voltage $V_s(t)$, (b) Estimated current $I_a(t)$, (c) Load current $I_l(t)$, (d) Reference current $I_{rh}(t)$.

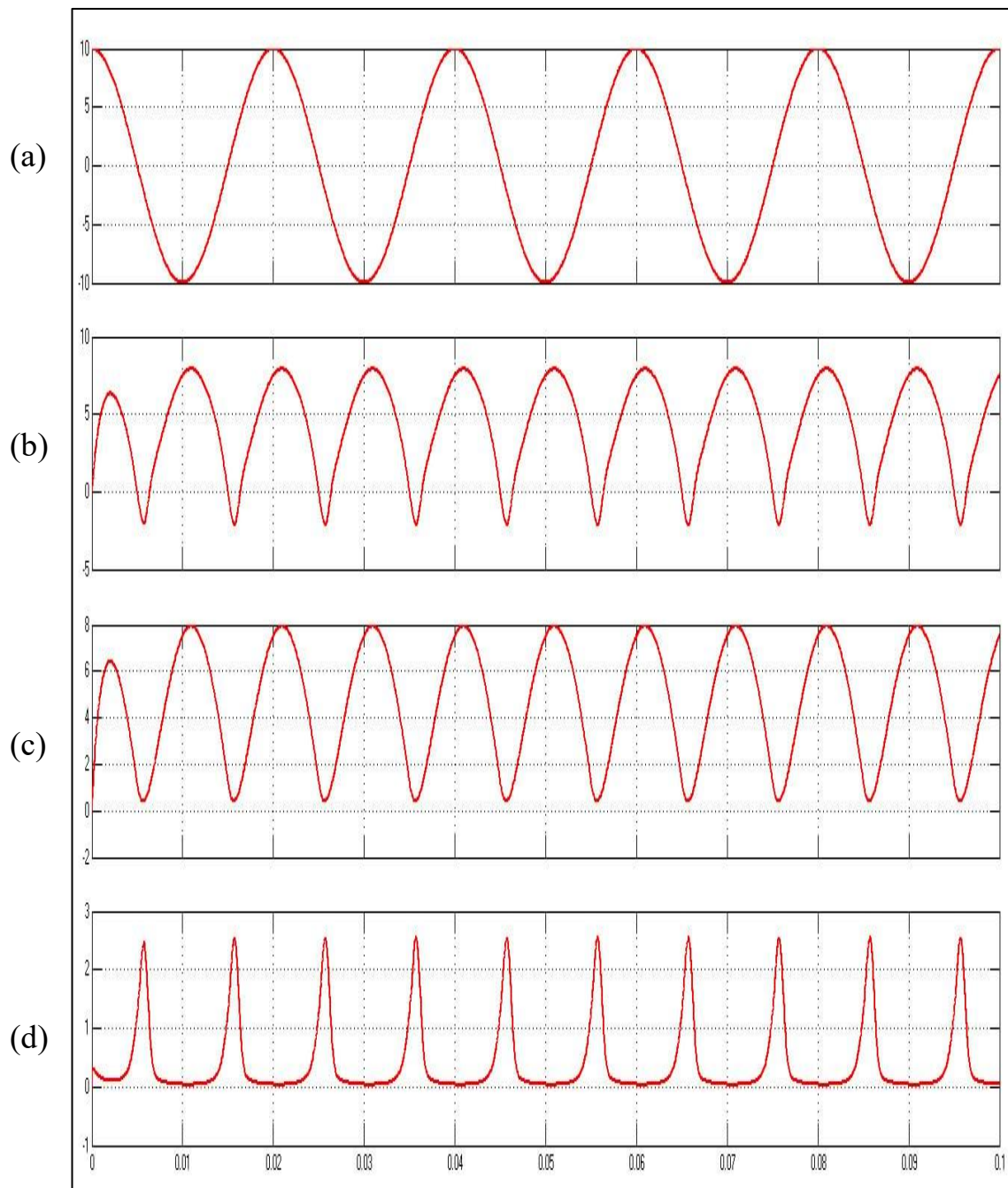


Fig 3.9: Simulation results for Full wave diodes rectifier with (RL-load), $f_s = 50$ Hz, (a) Mains voltage $V_S(t)$, (b) Estimated current $I_a(t)$, (c) Load current $I_l(t)$, (d) Reference current $I_{rh}(t)$.

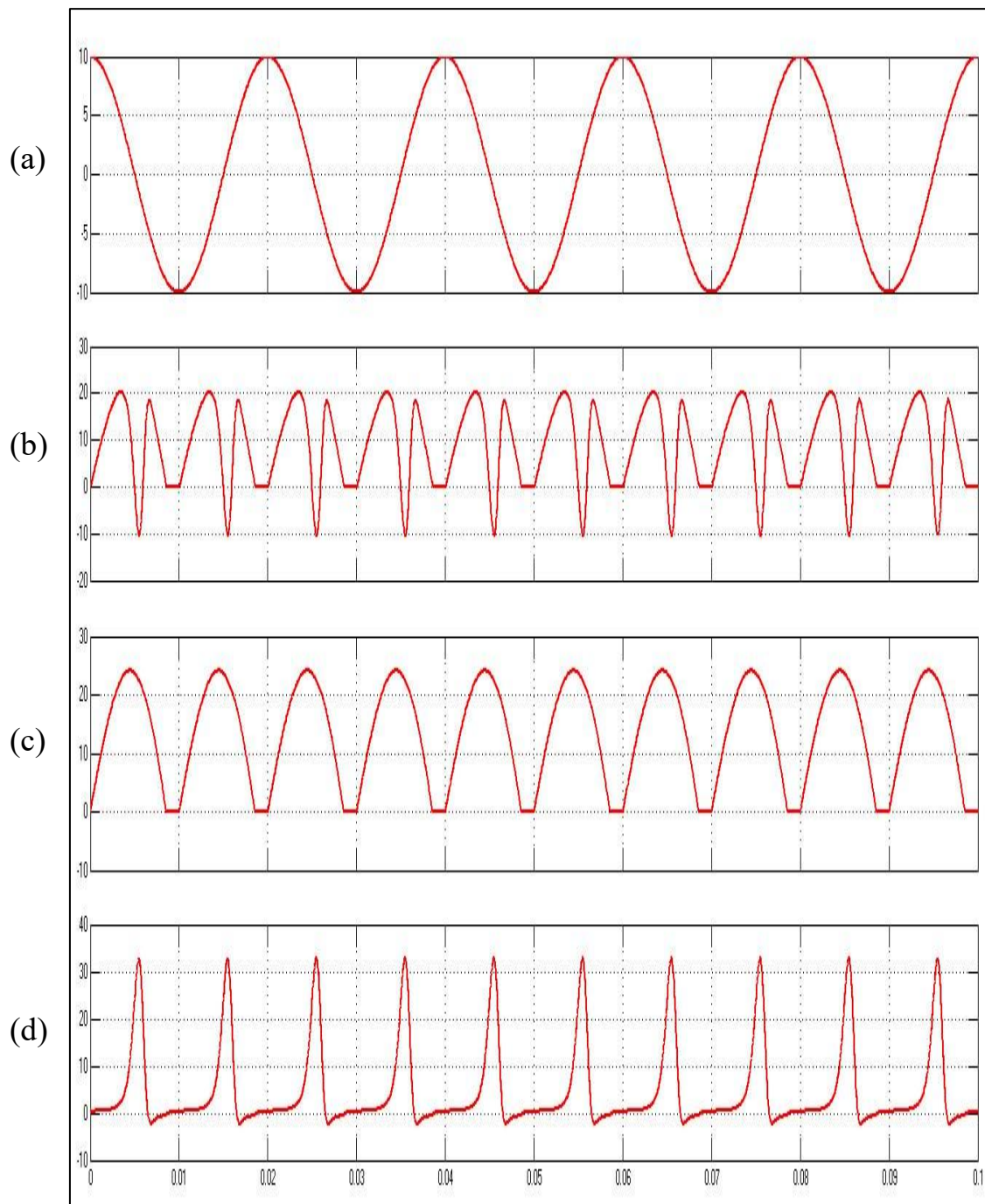


Fig 3.10: Simulation results for Full wave thyristor rectifier with (L-load) $f_s = 50$ Hz, (a) Mains voltage $V_S(t)$, (b) Estimated current $I_a(t)$, (c) Load current $I_l(t)$, (d) Reference current $I_{rh}(t)$.

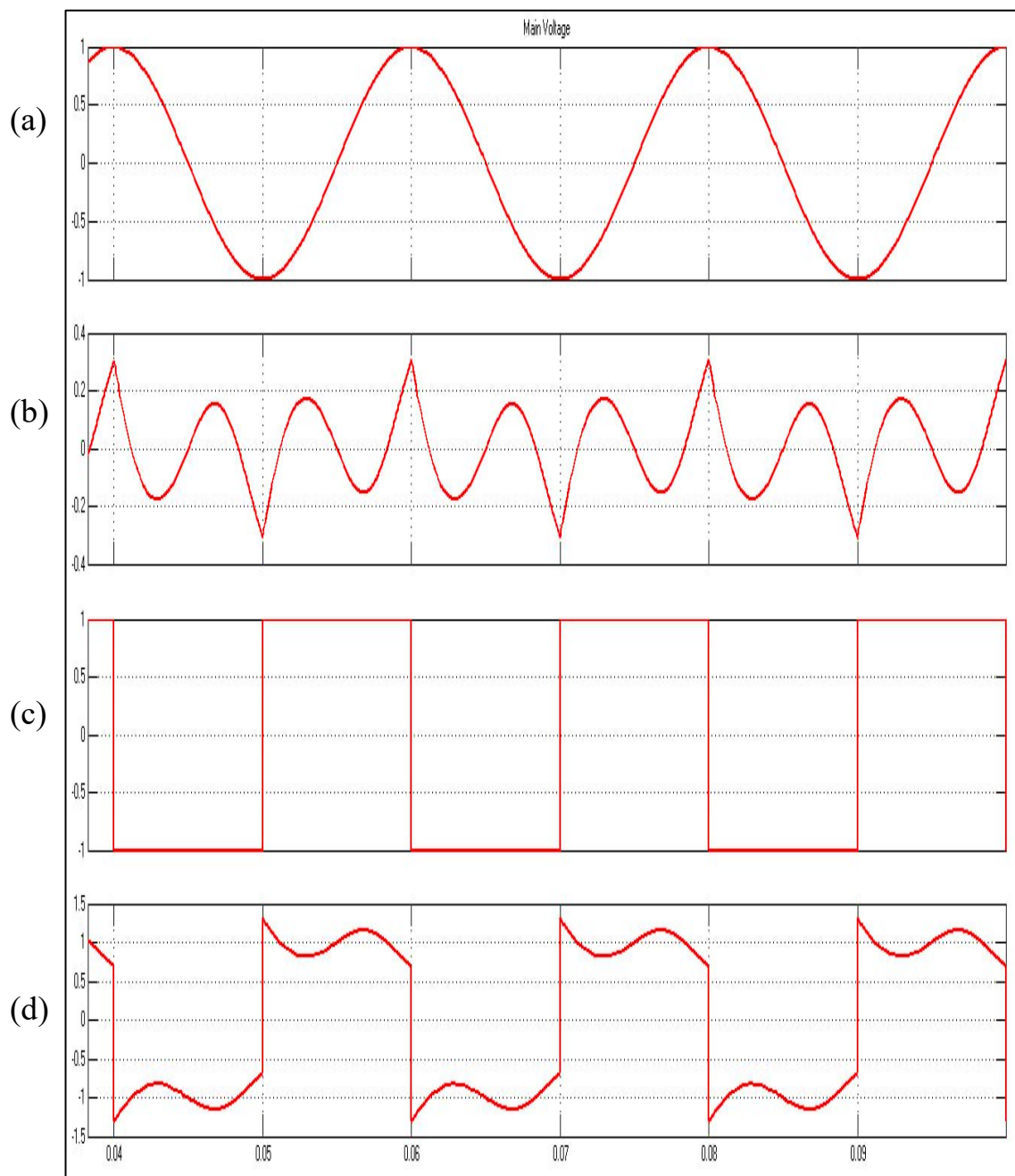


Fig 3.11: Simulation results for pure square wave, $f_s=50$ Hz, (a) Mains voltage $V_S(t)$, (b) Estimated current $I_a(t)$, (c) Load current $I_l(t)$, (d) Reference current $I_{rh}(t)$.

3.4 Conclusion

In this chapter, the implemented control circuit has been investigated, by simulations, for different trouble load conditions. The simulation results show that this control circuit can perform its job accurately and efficiently under all the assumed conditions such as the sudden change in the magnitude and phase of the load current, and under the condition of linear or nonlinear load.

This research has demonstrated the effectiveness of the estimated current method in enhancing the performance of Active Power Filters (APF) and improving power quality. Through MATLAB/Simulink simulations, the method proved capable of significantly reducing Total Harmonic Distortion (THD) while maintaining system stability under varying load conditions. The results highlight the advantages of this approach over conventional filtering techniques, particularly in its ability to adapt to dynamic changes and provide more accurate compensation for harmonic distortions.

A key finding of this study is the improved response of the APF when using the estimated current method. Unlike traditional techniques, which often struggle with transient conditions, this approach ensures better harmonic suppression and waveform quality. The comparative analysis further supports its effectiveness, revealing enhanced filtering efficiency and reduced steady-state errors. However, the research also underscores the importance of optimizing system parameters, such as switching frequency and DC-link voltage, to achieve the best performance. Despite its promising results, the method presents some challenges, particularly in terms of computational complexity and real-time implementation. Future research could focus on refining the algorithm to improve processing speed and accuracy. Additionally, practical testing, such as Hardware-In-the-Loop

(HIL) simulations, would be beneficial to assess its feasibility in real-world applications.

In conclusion, the estimated current method offers a powerful solution for APF control, significantly improving power quality and system efficiency. While further refinement is necessary, this study provides a strong foundation for future advancements in adaptive filtering techniques, paving the way for more reliable and effective power system applications.

CHAPTER FOUR

Conclusion And Future Work

4.1 Summary and conclusions

In this project, single phase active power filters have been studied and implemented. The proposed schemes employ a voltage source inverter to compensate for the reactive power requirement of the load current and eliminate the harmonic contamination caused by the nonlinear loads. Hence, the supply current will be a pure sinusoidal and in-phase with the supply voltage whatever the type of the load.

The theoretical and experimental investigations have shown that the implemented control circuit is fast and accurate in its response for all the studied cases. The electronic circuits used in implementation of the control circuits (such as PLL and multiplier circuits) are simple, accurate and have a fast response making an overall response time of about two cycles of the fundamental. Hence, simplicity, low cost and fast response are the main features of the implemented control circuit. The output current of the inverter used in the active power filter has been controlled according to the reactive and harmonic content of the load current. The tests carried out on the implemented APF have shown that its output current is effective in compensating the reactive and harmonic current of the load current for all the considered types of load (linear and non-linear with different power

factor). Almost unity power factor and sinusoidal mains currents have been obtained for the different types of loads used in these types.

The close agreement between analytical and experimental results proves the validity of the analysis and the feasibility of the proposed system. Finally, from analysis of the performance and practical results, it can be observed that the presented scheme has advantages of the conventional active power filter and overcome their problems.

4.2 Suggestions for future work

The following ideas may be suggested for future work in the field of APFs:

- **Artificial Intelligence & Machine Learning:** Using AI-based predictive algorithms to improve accuracy in detecting and compensating for harmonic distortions and reactive power.
- **Improved Filtering Techniques:** Replacing the low-pass filter with more advanced filtering techniques such as adaptive or Kalman filters for better noise reduction and faster response.
- **Digital Implementation using DSP or FPGA:** Implementing the entire control logic using Digital Signal Processors (DSPs) or Field-Programmable Gate Arrays (FPGAs) for faster processing and real-time control.

REFERENCES

- [1] J. B. Gupta, "Electrical Technology Vol.2", Katson Publishing House, Delhi-Ludhiana, section —VI- part-c/1, 1998.
- [2] Luis A.Moran, and Luciano Fernandez, Juan W. Dixon, and Rogel Wallace, "A simple and low-cost control strategy for active power filters connected in cascade", IEEE Transactions on Industrial Electronics, vol. 44, no. 5, pp. 621-629, October 1997.
- [3] T.J.E. Miller, "Reactive power control in electric systems" John Wiley & Sons, 1982.
- [4] Gyu-Ha Choe, and Min-Ho Park, "A new injection method for AC harmonic elimination by active power filter", IEEE Transaction on Industrial Electronics, vol. 35, no. 1, pp. 141-147, February 1988.
- [5] Elham B. Makram, Regan B. Haines, and Adly A. Girgis, "Effect of harmonic distortion in reactive power measurement", IEEE Transactions on Industry Applications, vol. 28, no. 4, pp. 782-787 July/August 1992.
- [6] Leszek S. Czarnecki, and Owen T. Tan, "Evaluation and reduction of harmonics distortion caused by solid state voltage controllers of induction motors", IEEE Transaction of Energy Conversion, vol. 9. no. 3, pp. 528-534, September 1994.
- [7] Peter Lynch, "An active approach to harmonic filtering". IEE REVIEW PP. 128-130, May 1999.
- [8] Philip T. Krein, "Elements of power electronic". New York Oxford. Oxford University Press, 1998.
- [9] P. Verdelho, and G.D. Marques, "An active power filter and unbalance current compensator", IEEE Transaction on Industrial Electronics, vol. 44, no. 3, pp. 321-328, 1997.

- [10] J. Sebastian Tepper, Juan W. Dixon, Gustavo Venegas, and Luis Moran, "A Simple frequency-independent Method for calculating the reactive and harmonic current in a nonlinear load", IEEE Transactions on Industrial Electronics, vol. 43, no. 6, pp. 647-653, December 1996.
- [11] Juan W. Dixon, Gustavo Venegas, and Luis Moran, " A series active power filters based on a sinusoidal current-controlled voltage source inverter", IEEE Transactions on Industrial Electronics, vol. 44, no. 5, pp. 612-919, October 1997.
- [12] Loszlo Gyugyi, "Reactive power generation and control by thyristor circuits", IEEE Transaction of Industry Applications, vol. IA-15, no.5, pp.521-534, September/October 1979.
- [13] Jin-He, and Ned-Mohan, "Switch mode VAR compensator with minimized switching losses and energy storage elements", IEEE Transactions on Power Systems, vol.5, no. 1, pp.90-95, February 1990.
- [14] David Nedeljkovic, Janez Nastran, Danijel Voncina, and Vania Ambrozic, "Synchronization of active power filter current reference to the network", IEEE Transactions on Industrial Electronics, vol.40, no. 2. pp. 333-339, 1999.
- [15] Fabiana Pottker de Souza, and Ivo Barbi, "Power factor correction of linear and non-linear loads employing a single-phase active power filter based on a full-bridge current source inverter controlled through the sensor of the AC mains current", IEEE, PESC, 99, pp.387-392, October 1999.
- [16] Simone Buso, Luigi Malesani, Paolo Mattavelli, and Reberto Veronese, "Design and fully digital control of parallel active filter for thyristor rectifiers to comply with IEC-1000-3-2 standards", IEEE Transactions on Industry Applications, vol. 34, no.3, pp.508-517, 1998.

- [17] W.M. Grady, M.J. Samotyj, and A.H. Noyola, "Survey of active line conditioning methodologies" IEEE Transactions on Power Delivery, vol.15, no.3, pp. 1536-1542, July 1990.
- [18] Leopoldo Rossetto, and Paulo Tenti, " Using AC-fed P WM converters as instantaneous reactive power compensators", IEEE Transactions on Power Electronics, vol.7, no. 1, pp. 224-230, January 1992.
- [19] Gyu-Ha Choe, and Min-Ho Park, " Analysis and control of active power filter with optimized injection", IEEE Transactions of Electronics, vol.4, no.4, pp. 427-433, October 1989.
- [20] Takeshi Furuhashi, Shigeru Okuma, and YoshiKi Uchikawa. "A study on the theory of instantaneous reactive power", IEEE Transactions Industrial Electronics, vol.37, no. 1, pp.86-90, February 1000.
- [21] Herofumi Acagi, Akira Nabue, and Satoshi Atoh, "Control Strategy of active filters using multiple voltage-source PWM converters". Transactions on Industry Applications, vol. IA-22. no pp.460-456. May/June 1986.
- [22] Hirofumi Akagi, Yoshihira Kanazawa, and Akira Nobae, "Instantaneous reactive power compensators devices without energy storage components" IEEE Transactions on Industry Applications, vol. IA-20, no.3, pp.625-630, May/Juen 1984.
- [23] T. Moran, Phoivos D. Ziogas, and Geza Joos, "Analysis and design of a novel 3-phase solid-state power factor compensator and harmonic suppress or system", IEEE Transactions on Industry Applications, vol.25, no.4, pp.609-619, July/August 1989.
- [24] Fang-Zhang Peny, Hirofomi Akagi, and Akira Nabae, "A study of active power filters using quad-series voltage source PWM converters for harmonic compensation", IEEE Transactions on Power Electronics, vol.5, no. 1, pp.9-15, January 1990.

- [25] J. -C. Wu, and H. -L. Jou," Simplified control method for the single-phase active power filter", IEE Proc, Elec. Power Appl., vol.143, no.3, pp.219-224, May 1996.
- [26] Martin F. Schlecht, " Harmonic-free utility IDC power conditioning interfaces", IEEE Transactions on Power Electronics, vol. PE-I, no.4. pp. 231-239, October 1986.
- [27] M. Azizur Rahman, Tawfik S. Radwan, Ali M. Osheiba, and Azza E. Lashine, "Analysis of current controllers for voltage-source inverters", IEEE Transactions on Industrial Electronics, vol.44s no.4, August 1997.
- [28] M. H. Rashid, "Power electronics, circuits. devices and application". Prentice-Hall International Editions Inc., 1988.
- [29] B.W. Williams, "Power electronics, devices, drivers and applications". Macmilar Education LTD, 1987.
- [30] Y. H. Kim, and M. "Ehsani, Discussion of an algebraic algorithm for Microcomputer based (direct) inverter pulse width modulation", IEEE Transactions on Industry Applications, Vol .24, no.6, pp.998-1003, November/December 1988.
- [31] Raymon S. Ramshaw, Guoliang Xie, Barry W. Henderson, and Johan H. Degroot, "A P WM inverter algorithm for adjustable speed Ac drives a non-constant voltage source", IEEE Transactions on Industry Applications, vol. IA-22, no.4, pp.673-671, July/August 1986.
- [32] Keiji Matsui, Tadashi Yamaguchi, and Shinichi Takase, "A novel PWM strategy to minimize the surge voltage for current-source converters", IEEE Transactions on Industry Applications, vol.34, no.3, pp.501-507, May/June 1998.
- [33] Tashihiko Noguchi, Hiroaki Tomiki, Seiji Kondo, and Isao Takahashi, "Direct power control of P WM converter without power-source voltage

sensors", IEEE Transactions on Industry Applications, vol. 34, no.3, an-479. May/June 1998.

- [34] I.J.Nagrath, and M.Gopal, "Control systems engineering ", New Age International Publishers, New Delhi, 3 rd edition, 2000.
- [35] David L. Blackburn, "Turn-off Failure of Power MOSFET" IEEE Transactions on Power Electronics, vol. PE-2, no.2, pp. 136-142. April 1987.
- [36] Howard M. Berlin, "Design phase-locked-loop circuits, with experiments", Howard W. Sams Co., Inc., 1986.
- [37] George Loveday, "Essential Electronic", Oitman Book limited, 1982.
- [38] Ramakant Gayakwad, and Leonard Sokoloff, " Analogue and digital control systems", Prentice-Hall International, Inc., 195-199, 1988.

APPENDIX A

The 565 PLL

A-1 The complete configuration of the NE 565 phase locked loop (PLL) is shown in fig. A-1. It is a self-contained, adaptable filter and demodulator for the frequency range from 0.001 Hz to 500 KHz. This circuit comprises a voltage-controlled oscillator, phase comparator, amplifier and low-pass filter shown in the block diagram. The center frequency of the PLL is determined by the free running frequency of the VCO, this frequency can be adjusted externally with a resistor (R_1) or a capacitor (C_1).

A-2 Absolute maximum ratings

Operating voltage	26v
input voltage	3v p-p
power dissipation	300mw

A-3 Design Formulas

$$\text{Free running frequency of VCO} = \frac{1.2}{4R_1C_1} \text{ in Hz}$$

$$\text{Lock-range } f_L = \pm \frac{8f_0}{V_{cc}} \text{ in Hz}$$

$$\text{Capture-range } f_C = \pm \frac{1}{2\pi} \sqrt{\frac{2\pi f_L}{r}}$$

$$r = 3.6 \times 10^3 \times C_2$$

APPENDIX A

A-4 Block Diagram

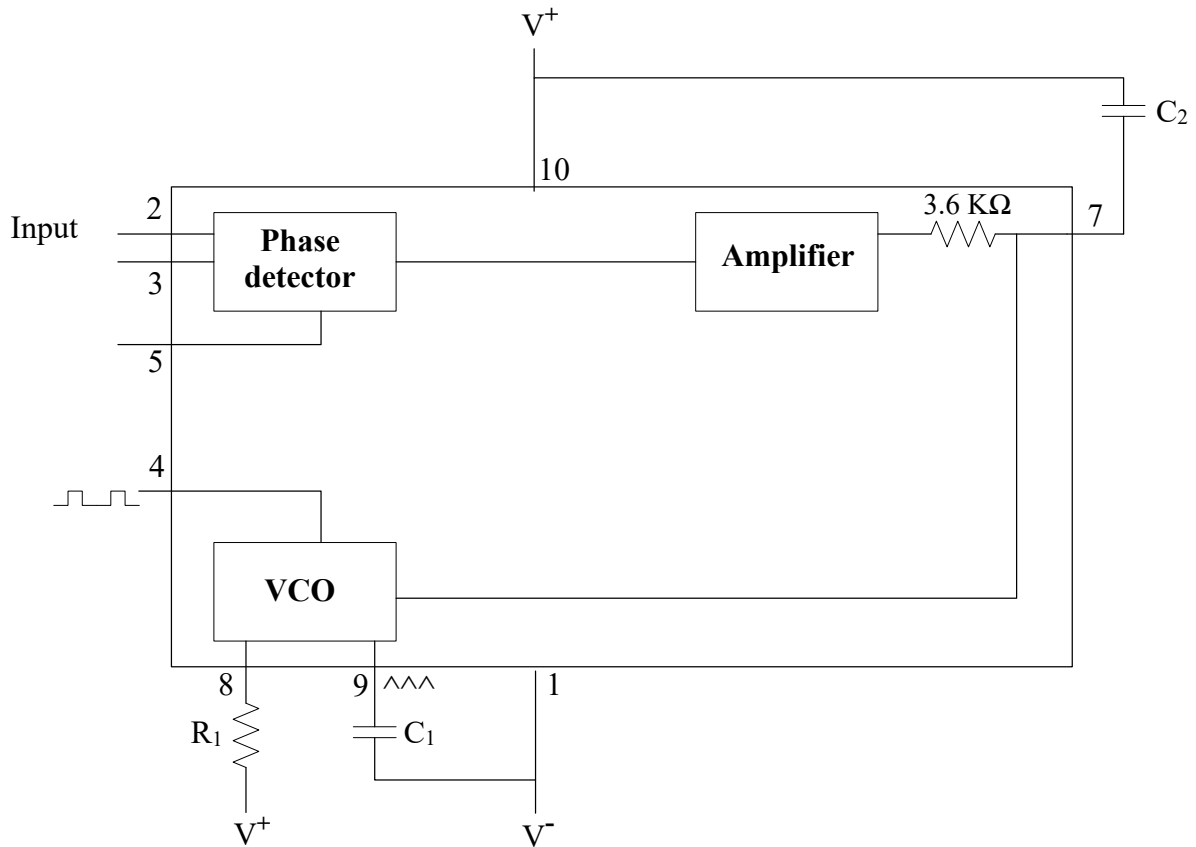


Fig (A-1): Block diagram of PLL.

APPENDIX B

Selection of the LPF elements

The transfer function of the first order LPF, shown in Figure B-1, is:

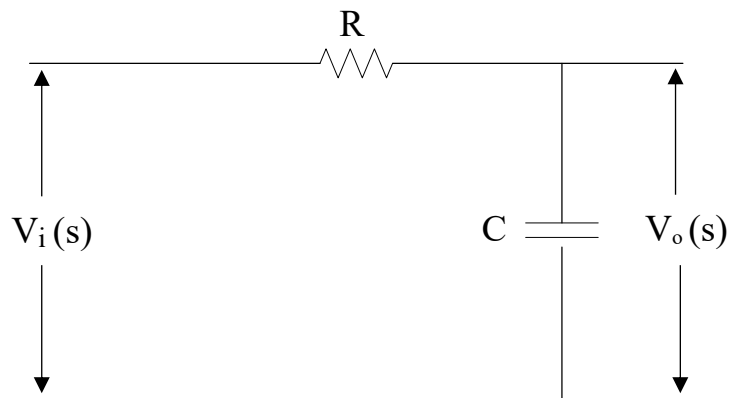


Fig. (B-1): First order LPF.

$$\begin{aligned}\frac{V_i(s)}{V_o(s)} &= \frac{1/RC}{s + 1/RC} \\ &= \frac{\omega_0}{s + \omega_0}\end{aligned}\tag{B-1}$$

where $\omega_0 = \frac{1}{RC}$ is the cut-off frequency of the filter.

choosing $\omega_0 = 20\pi$ rad/Sec. yields

$$\text{for } R = 1.5 \text{ K}\Omega$$

$$C = 106 \mu\text{F}$$

APPENDIX C

Selection of the P-I controller elements

The transfer function of this controller:

$$G(s) = K_p + \frac{K_1}{s}$$

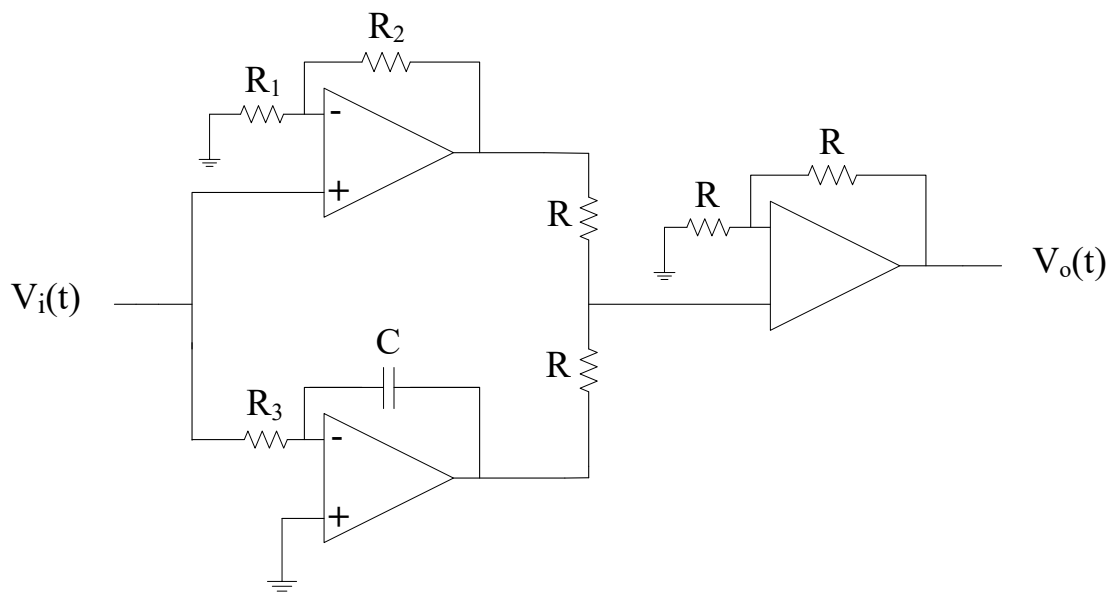


Fig (C-1): P-I controller.

The parameters of this controller have been elected in section (3.5. 1) as ($K_p = 35$ and $K_r = 400$) to obtain optimal response of the system.

From Figure (C- 1).

$$K_p = 1 + \frac{R_1}{R_2}$$

Let $R_1 = 34 \text{ K}\Omega$ then $R_2 = 1 \text{ K}\Omega$

Also, $K_1 = \frac{K_p}{R_3 C}$

Let $R_3 = 1.5 \text{ K}\Omega$ then $C = 10 \mu\text{F}$

الخلاصة

يتناول هذا البحث تصميم دائرة سيطرة لمرشحات القدرة الفعالة. (Active Power Filters) , هذا الفلتر يستخدم في تحسين جودة الطاقة الكهربائية من خلال تعويض القدرة غير الفعالة وإزالة التوافقيات. تم تحليل أداء المرشحات النشطة الأحادية والثلاثية الطور، مع استخدام تقنيات التحكم في التيار والجهد القائمة على تعديل عرض النبضة. (PWM) تمت دراسة استجابة المرشح في حالة الاستقرار (Steady State) ، وتأثير التغير في تيار الحمل ذي معامل القدرة الموحد (UPF) ، إضافة إلى تحليل تأثير الأحمال غير الخطية على كفاءة المرشح. كما تم تقييم أداء المرشح تحت تغيرات مختلفة في الحمل، مع الأخذ في الاعتبار أن التردد المستخدم في جميع الاختبارات هو 50Hz، وتم ضبط التحكم باستخدام نظام قفل الطور. (Phase-Locked Loop) تم التحقق من كفاءة المرشح النشط من خلال المحاكاة الحاسوبية باستخدام برنامج MATLAB/Simulink. شملت المحاكاة دراسة سلوك النظام تحت ظروف تشغيل متعددة، مع التركيز على تقليل التشوه الكلي للتوافقيات (THD) وتحسين معامل القدرة. أظهرت النتائج أن مرشحات القدرة النشطة تعمل بكفاءة في تقليل التوافقيات وتعويض القدرة غير الفعالة، مما يساهم في تعزيز استقرار وكفاءة الشبكة الكهربائية.



جمهورية العراق
وزارة التعليم العالي والبحث العلمي
جامعة ميسان
كلية الهندسة
قسم الهندسة الكهربائية



تصميم دائرة سيطرة لمرشحات القدرة الفعالة

بحث تخرج

مقدم الى قسم الهندسة الكهربائية في كلية الهندسة جامعة ميسان كجزء من متطلبات الحصول على
درجة البكالوريوس في الهندسة الكهربائية

اعداد

جعفر محمد صالح

عباس علي خماس

سجاد حسن مذبوب

بنين حسن هاشم

بإشراف

الأستاذ المساعد الدكتور جبار رحيم راشد

Misan, Iraq

2025